SYNTHESIS OF Zn-DOPED ZEOLITES FOR ENHANCED PHOTOCATALYTIC ACTIVITY

Submitted by
FATIMA NADEEM
MSCHE-S22-013

Supervisor: Dr. Fizza Naseem

Co-Supervisor: Dr. Shaista Ali

M.Phil. Chemistry

Department of Chemistry
Faculty of Sciences
The Superior University, Lahore
2023

UNDERTAKING BY STUDENT

I Fatima Nadeem Regd.No. MSCHE-S22-013 declares that the content of my research synopsis entitled "Synthesis of Zn doped zeolites for enhanced photocatalytic activity" is based on my research findings and has not been taken from any other work except the references and has not been published before.

Fatima Nadeem

Department of Chemistry

Faculty of Sciences

The Superior University, Lahore

SUPERVISOR CERTIFICATE

I have thoroughly reviewed the synopsis of Fatima Nadeem Reg. No. MSCHE-S22-013 for MPhil Chemistry Session (2022-2024) on the topic "Synthesis of Zn doped zeolites for enhanced photocatalytic activity."

I found it satisfactory for the final submission.

20th August 2023

Dr. Fizza Naseem
Ph.D. Chemistry
Assistant Professor
Department of Chemistry

Department of Chemistry
Faculty of Sciences
The Superior University, Lahore

APPROVAL LETTER ETHICS REVIEW COMMITTEE

Synopsis entitled “Synthesis of Zn-dopped zeolites for enhanced photocatalytic activity” Submitted by Fatima Nadeem under Roll No. MSCHE-S22-013 has been approved for research work.

	Dr. Uqba Mehmood Convener-Research Review Board	
Dr. M. Mudassir Iqbal (Member)	Dr. Hina Zain (Member)	Dr. Sumyyia Abrar (Member)

Department of Chemistry

Faculty of Sciences

The Superior University, Lahore

Table of Contents

SYNTHESIS OF Zn-DOPED ZEOLITE FOR ENHANCED PHOTOCATALYTIC ACTIVITY

ABSTRACT

Water is one of life's most important needs and is necessary for humans to survive in the environment. Even though water is abundant on Earth, just 1.7% of it is freshwater that can be used to meet human requirements. Unfortunately, pollutants that are constantly released into aquatic bodies damage freshwater. Dye-containing textile unit discharge is one of these concerning pollutants. Dye contamination of water causes major health problems (mutagenicity, cancer) and disrupts aquatic life (eutrophication, decreased light penetration). Because of their resilience and intricate structure, dyes are hard to remove with traditional techniques. The steps that are used to eliminate dyes are as follows: Biological, chemical, and physical. Because of their limitations, all of these tactics have little use. Therefore, contemporary dye degrading techniques should be investigated. AOPs, which are based on the generation of OH• radicals with a potent oxidizing capacity to break down a variety of contaminants, are one such technique that has drawn a lot of interest. One of the most popular AOPs for water remediation is photocatalysis, which employs catalysts (mainly semiconductors) to accelerate deterioration by producing more radicals. In addition to being a semiconductor photocatalyst, ZnO-NPs have found many other uses because of their remarkable qualities. They are frequently used in photo detectors, solar cells, and optical gas sensors. ZnO-NPs are proven to be exceptionally effective at degrading a wide range of contaminants, such as organic pollutants, synthetic colors, and pharmaceutical waste. Given the growing need for creative, environmentally friendly, and sustainable water treatment methods as well as its noteworthy characteristics and intricate structure that enable it to hold ions and particles and let light in, reach, and interact with them all of which are crucial as photocatalyst activators zeolite is regarded as a leading contender. Zeolite activity was enhanced by doping with zinc metal and used for the degradation of three model dyes MO, MB, and CR with degradation efficiency 96%, 98.4%, and 99.8%.

CHAPTER-1INTRODUCTION

1.0 INTRODUCTION

Water is the most plentiful and valuable material in the geosphere, making up over 3/4 of it. There are three distinct states of water in the environment: solid, gas, and liquid. At room temperature, the liquid is almost colorless, with a little blue tint, and has no taste or smell. Because it dissolves so many substances, water is frequently referred to as the universal solvent(1). Water is also an essential component of the human body. It usually accounts for 60% of an adult male's body weight, while it is much lower (50–55%) in females due to their greater body fat percentage. About 71% of the liver, 22% of the bones, 20% of adipose tissue, 75% of the brain and muscles, and 81% of the blood and kidneys are composed of water. Enough water is necessary for the body to survive and operate. Although people may disregard other vital elements for weeks or months, they cannot envisage their lives without water, depending on many factors (such as the level of effort, humidity, and other conditions)(2). Even though water is largely cleaned, no nutrient on Earth can completely replace it. Water is utilized for many purposes outside drinking, such as cooking, food processing, industrial processes, agriculture, energy generation, and the production of steel for vehicles. Because of its profound effects on the body, water is referred to as the "heart of life." Social and economic well-being are unquestionably reliant on this renewable resource. Earth has a lot of water (70–80%), but only 3% of it is freshwater (found in glaciers, groundwater, running surface water, etc.), and the remaining 97% is seawater, which is too salty to be used for anything(3). Additionally, 0.36% of the fresh water is usable; the remainder is found in polar ice caps, subterranean wells, and aquifers, as seen in Fig 1. Groundwater is essential for drinking for one-third of the world's population(4).

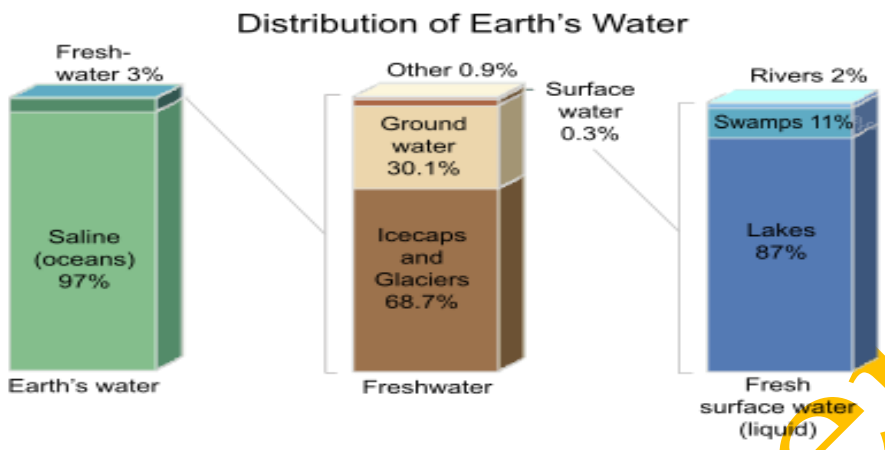

Figure 1. World's Distribution of water

Freshwater supplies are unfortunately depleted quickly because of unchecked resource use, rapid industrialization, growing urbanization, and human and governmental dominance. Currently, around 80% of people on the planet cannot use or drink clean water(5).

1.1 Water Pollution

When undesired and unwanted elements are added to water, it becomes unsuited for use in many activities including drinking, cooking, bathing, and other activities. This is known as water pollution. It is an international issue that has a negative impact on water quality. Hepatitis, diarrhea, cholera, jaundice, and cancer are among the waterborne illnesses brought on by drinking contaminated water. The most common source of water contamination is human activities(6). Deforestation, littering, fertilizers, pesticides, heavy metals, oil spills, waste from industry sites, sewage leaks, animal and chemical wastes, and other sources are the main sources of pollutants discharged into the environment. Various natural and man-made chemical contaminants are among the pollutants produced by these businesses, which utilize around one-third of the available renewable freshwater. As many countries, like Pakistan, enter industrial revolutions, water contamination is becoming a more serious problem. Water contamination in developing countries is frequently caused by pollution issues associated to the textile industry, as it is one of the primary causes of pollution in these regions(7). These industries are primarily responsible for the discharge of coloring chemicals and colorants. Only a few other industries employ these colors, including the sugar, paper, and leather tanning sectors. The textile industry has been around for 4,000 years. Textile dyeing and the fermentation of sugar to make alcohol are two well-known and ancient businesses. By oxidizing animals, William E. Perkin produced

the first synthetic color in 1856. Today, more than a thousand synthetic dyes are available for purchase, and tens of thousands are created. The textile industry employs the vast bulk of synthetic dyes produced. The use of synthetic dyes has increased dramatically in many facets of our everyday life and will only increase in industries such as development, painting, paper, leather, and cosmetics. Nearly 10,000 distinct dying colors are used in various sectors(8). An astounding 0.7 million tons of coloring compounds are produced annually worldwide. The main consumer of these dying ingredients is the textile sector, which utilizes 3×10^5 tons of dyeing chemicals which harmfully impact human health and environment as shown in fig 2

Figure 2. Water pollution caused by dyes and printing inks

1.2 Dyes Toxicity

One of the most prevalent organic contaminants among the untreated chemicals released by the textile industry are textile dyes. Azole dyes, which structurally consist of one or more azo groups, are the most prevalent class (over 60%) of all textile dye groups. Additionally, these are the dyes that are most often used. In the field of textile. Due to inadequate textile dyeing techniques, 15–50% of azo dyes that are not bonded to fibers and textiles are discharged into wastewater. While some textile manufacturers treat their wastewater to break down free azo dyes that are released into the environment, others release untreated industrial(9). Because of subpar textile dying techniques, 15–50% of azo dyes that are not bonded to fibers and textiles end up in wastewater. While some textile companies treat their wastewater to remove free azo dyes from

the environment, others dump untreated industrial waste into bodies of water, which can have negative effects on living things and present serious ecological and toxicological dangers(10). Human exposure to colored effluents caused a variety of immune suppression symptoms, signals of neurobehavioral issues, heart disease. Central nervous system, airborne, and allergy symptoms, such as lung edema, cancer, and cyanosis(11).

1.3 Importance of dye Removal

Usually, dye-using enterprises stock dye discharge as industrial trash after dyes have completed coloring items. These contaminants are then discharged into habitat water bodies, converting clear, colorless water into contaminated, colored water. Wastewater with colors and pigments is not only ugly, but it also offers serious health hazards, including diarrhea, bleeding, and other water-borne infections; eye damage; carcinogenic, mutagenic, and genotoxic effects; neurotoxicity; endocrine disruption; liver damage; and allergies(12). They also harm the ecosystem by decreasing light penetration, raising the need for biochemical oxygen, interfering with photosynthetic activity, inhibiting plant development, and decreasing the food chain of aquatic creatures. Additionally, dye effluents change the chemical and physical characteristics of arable soil. Sulfur (S), hydrogen (H), nitrogen (N), and carbon (C) elemental profiles alter after being subjected to textile dyes. Therefore, it is imperative that substantial measures be implemented to stop the accidental discharge of textile dyes into the environment(13). It seems that having suitable, reasonably priced treatment methods for polluted wastewater is crucial. Most photo catalytic investigations just use one test dye solution's degradation. It is quite challenging to purify water since real industrial effluent usually comprises a mixture of organic hues(14).

1.4 Dyes Treatment Methods

The fundamental human right is access to clean water, yet human activity and undone approaches make this impossible. According to estimates, by 2030, 47% of the world's population would face a shortage of drinkable water. Waste water treatment has been the subject of several studies employing various etymologies(15). One of the three types of dye removal methods used nowadays is

1. Physical operations.
2. Biological Operations
3. Chemical Operations

The complex structure of dye effluents means that no one treatment method is as successful in handling dye wastewater. To offer the required water quality, several strategies are applied effectively.

1.5 Physical Operations

Visible dye degradation processes are often carried out via the diffusion-controlled process. Physical methods that are commonly used include irradiation, reverse osmosis, membrane filtration, aggregation or flocculation, ion exchange, adsorption, and nano- or ultra-filtration. The clear design, ease of use, low cost, little chemical needs, and absence of resistance in the form of dangerous contaminants are only a few advantages of physical approaches. However, because of some drawbacks, such as the production of sludge and dangerous materials, and limited application, these processes are generally not advised(16).

1.6 Biological Operations

It is a viable technology for cleaning industrial effluents since biological dye removal has benefits over traditional treatment techniques. Their benefits include ease of use, reduced residue production, minimal chemical requirements, cost-effectiveness, low energy consumption, sustainability, and non-toxic byproducts from microbial metabolism. Yeast, fungus, bacteria, algae, and enzyme-based systems are biocompatible options for purifying industrial waste that contains colors(17). Dye compounds can be changed into innocuous chemicals by these microbes. Consuming ubiquitous microbes is the main advantage of biotic methods. Their ability to thrive in even the most polluted surroundings and their resilience to hardship make them an attractive pot for studying interesting catalysts and materials that may be employed to lessen ecological concerns. The many functional groups found in microbial cell walls, such as amino, phosphate, carboxyl, and hydroxyl, are responsible for the attraction between the color of contaminated water and the microbial cell wall(13, 18).

1.7 Chemical Operations

To get rid of garbage that contains dyes, chemical procedures employ chemical science or its principles. Chemical methods such as electrochemical, photochemical, Fenton, and ozonation are used to treat wastewater that contains dyes. Most of these methods are more expensive than the other two, with the exception of the electrochemical dye removal method(19). In addition, the environmental effects, the amount of chemicals required, the equipment required, and the high energy needs are the main disadvantages of adopting chemical techniques for the commercial

color removal of textile effluent. Utilizing these techniques carries additional danger due to the unstable materials and byproducts created during the treatment procedure(20).

1.8 Advanced Oxidation Processes (AOPs)

In the filtration and treatment of water, AOPs have shown great potential, particularly in the elimination of pesticides and other dangerous substances. These pollutants are becoming more of an issue. Glaze's definition of AOPs as processes that "involve the production of hydroxyl radicals in desirable quantity that affect water purification" was one of the earliest uses of the term. The idea behind AOPs has evolved since the 1990s, and they are now used to create hydroxyl radicals and other reactive oxygen species, such as hydrogen peroxide, singlet oxygen, and superoxide anion radicals(21). Additionally, the OH is still the species most associated with the effectiveness of AOPs. Most organic molecules interact with hydroxyl radicals via addition or hydrogen abstraction to produce carbon-centered radicals. The carbon-centered radical that is formed when the peroxyl radical interacts with molecular oxygen to produce a variety of oxidation products includes alcohols, aldehydes, and ketones. The methods used in AOPs include typically electrochemical oxidation processes, Fenton, photo-fenton, ozonation, and homogeneous and heterogeneous photocatalysis(22). These methods can remove color quickly and without sludge accumulation in challenging situations. They do, however, have certain disadvantages, like being expensive, needing a specific pH, and producing dangerous byproducts. Among all of these methods, heterogeneous photocatalysis has received far too much attention since Honda and Fujishima carried out the first photo-catalyzed AOP based on titanium oxide (TiO_2) in 1972.

1.9 Photocatalysis

"Photocatalysis" is a combination of the words "photo," which means "light," and "catalysis," which is the reaction of a decomposing reactant with an agitator to change the rate of a reaction. The first photo-catalyzed AOP based on titanium oxide (TiO_2) was carried out in 1972 by Honda and Fujishima. It is known for being a technology that is environmentally friendly, energy-efficient, and sustainable. High levels of pollution, high complexity, and low biodegradability are all efficiently treated by this method. Organic dyes may be completely mineralized into H_2O, CO_2, and mineral acids by photocatalysis without producing secondary pollutants(23).

1.10 Principle of Photocatalysis

During photocatalysis, four fundamental stages take place.

1. Picking blaze
2. The division of charges
3. Charge flow (perhaps recombination)
4. Use of charges for redox processes

Whereas excited electrons on a CB jump to a VB when light reaches a certain energy, holes stay on a VB. On the surface of the photocatalyst, the hole of VB facilitates an oxidation process, whereas the electrons of CB cause a reduction reaction. The holes in this reaction oxidize OH^- to •OH, which has the effect of breaking down contaminants. When h^+ and dissolved O_2 are present in the aqueous solution, the electrons cause H_2O_2 or superoxide radicals (O^{2-}) to form(24), as seen in Fig 3.

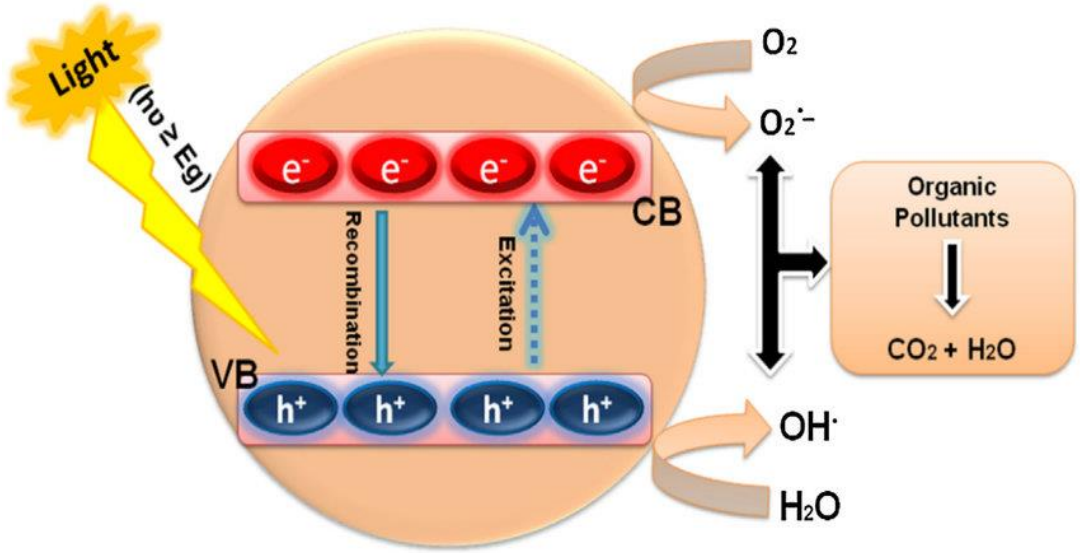

Figure 3 Mechanism for Photocatalysis

1.11 Photocatalysis using Zeolites

The investigation of photocatalysis has emerged as a promising avenue for addressing environmental contamination and facilitating the production of renewable energy. Photocatalysts driven by semiconductors have significant interest due to their ability to harness solar energy to initiate photochemical reactions(25). Among these semiconductor-driven photocatalysts, zeolites have emerged as particularly intriguing candidates because of their special qualities. Zeolites possess a high surface area, well-structured pore arrangement, and a customizable framework

composition, which make them highly versatile for various applications. These attributes allow zeolites to efficiently adsorb and catalyze target molecules, making them ideal candidates for environmental remediation, pollutant degradation, and renewable energy generation(26).

The Greek terms "zeo: boiling" and "lathes: stone" are the origin of the word "zeolite," which generally refers to boiling stones. Swedish mineralogist Axel Fredrik Cronstedt first described this in 1756 after learning of their intumescence characteristics. He discovered that the mineral's vapor was released as water evaporated because of heating. Following that, the rapid loss of water gave the impression that the zeolite material was boiling. Heat-induced dehydration of zeolites results in many empty spaces, where the so-called "molecular sieve" is formed in the zeolite's adsorbent characteristics. Only molecules smaller than or equal to the size of the cavity can pass through channel holes in molecular sieves; molecules larger than the size of the pores are not allowed. The internal zeolite was adsorbed to gas or liquid molecules that were tiny enough to fit through the entrance channel after dehydration; bigger molecules were an exception(27). The main component of all zeolites is an alumina-silicate structure that consists of four anions of oxygen (O_2^-) encircling a tetrahedral arrangement of silicon (Si^{4+}) and aluminum (Al^{3+}) cations. AlO_2 and SiO_2 rectangular blocks form a three-dimensional macromolecular structure when each oxygen ion in the Al–O and Si–O bonds two cations and is shared by two tetrahedrons. Zeolites are known to have basic and acid sites, and they exhibit amphoteric characteristics. For the purpose of creating effective photocatalytic systems, zeolite provides a large surface area, a distinct nanoscale porous structure, and ion exchange capabilities. The 13 Å super-cages that make up the structure of pores of zeolite-Y are joined by 7 Å windows. Zeolites are said to offer particular photophysical characteristics, namely the regulation of electron and charge transfer mechanisms. Due to their ionic exchange ability, zeolites may also be advantageous in photocatalysis(28).

1.12 Limitations of Zeolite as photocatalyst

Although zeolites offer numerous advantages, their intrinsic limitation lies in their

- Wide bandgap, which restricts their photocatalytic performance primarily to UV light
- Constituting only a small fraction of the solar spectrum.

1.13 Modifications of Zeolite with Metals

Recognizing the above-mentioned challenge and seeking to expand the applicability of zeolites in visible light photocatalysis, scientists have focused their efforts how to improve the activity of

zeolites. There are various options for zeolite modifications like composite formation, doping, and supported zeolite. Among all above mentioned options doping is the best choice because doping improved chemistry; for example, larger crystal sizes and increased surface area lead to a high degree of crystallinity, changes in electronic structure, which raises photo-catalytic efficiency and decreases charge separation in photo-induced e^{-}/h^{+} pair recombination(29). Additionally, the tunable framework composition of zeolites enables the incorporation of dopants, which can further enhance their photo catalytic activity by modifying their electronic structure and surface properties.

As a result, the synthesis and optimization of doped zeolites have become a focal point of research in the field, aiming to develop efficient and sustainable photocatalysts for diverse applications in environmental and energy-related sectors. Through systematic investigation and optimization of synthesis methods, characterization techniques, and photocatalytic performance evaluation, researchers aim to unlock the full potential of doped zeolites and propel the field of photocatalysis towards practical implementation for a cleaner and more sustainable future.

Different metals have been used for the modification of zeolites. Among these metal ions, zinc has become an especially promising candidate due to its peculiar electronic and structural characteristics. By introducing zinc into the zeolite structure, researchers aim to modify the optical properties of zeolites, thereby extending their photocatalytic activity within the spectrum of visible light. The incorporation of zinc ions offers opportunities to tailor the bandgap of zeolites, enabling absorption of visible light photons and facilitating photoinduced electron transfer processes. Furthermore, zinc doping can induce changes in the surface chemistry and electronic structure of zeolites, leading to improved charge separation and migration, which are crucial factors for enhancing photocatalytic efficiency. Through careful design and optimization of zinc-doped zeolites, scientists seek to harness the abundant solar energy available in the visible light spectrum for driving photocatalytic reactions efficiently. In addition to addressing the intrinsic drawbacks of zeolites, this line of inquiry advances the creation of environmentally benign and sustainable photocatalytic materials with a wide range of uses in fields like solar energy conversion, water purification, and environmental remediation.(30). This property can be used to incorporate transition metal ions, which exhibit significant photocatalytic activities because of their unoccupied d-orbitals(31). The successful fabrication of zinc-incorporated zeolites without the use of a template has also been demonstrated, exhibiting improved

photocatalytic activity in reduction processes. Even though this research has made significant strides, systematic investigations are still required to improve the sol-gel production method and the ideal zinc doping concentration in order to further boost the photocatalytic capabilities of zeolites. Fine-tuning the concentration of zinc dopants is essential to achieve the desired balance between increased photoactivity and minimized recombination of photoexcited charge carriers. Additionally, optimizing the sol-gel synthesis parameters, such as precursor ratios and reaction conditions, can lead to the controlled formation of ZnO nanoparticles within the zeolite framework, ensuring improved photocatalytic efficiency and long-term stability. Comprehensive investigations into these factors will contribute to advancing our understanding of the mechanisms underlying zinc-mediated photocatalysis in zeolites and open the door for the creation of sustainable and incredibly effective photocatalytic materials for environmental remediation and energy conversion applications (32).

1.14 Aims and Objectives

By altering zinc-doped zeolites, the study aims to increase their photo catalytic activity when exposed to visible light. The particular objectives will be defined as follows

- To create a photocatalyst doped with zeolite and containing different amounts of ZnO
- To evaluate the synthesized photocatalysts' morphological and configurational features.
- To examine how well the modified zeolites operate photo catalytically to degrade dyes making water usable for poeple

1.15 Problem Statement

Because of their wide energy gap, zeolites are not suitable for solar-powered applications. Unfortunately, the photo catalytic efficiency of zeolite is mostly limited to UV light. To overcome this problem, this study introduces a novel photocatalyst that consist of ZnO-doped zeolite This modification increase the ingestion of visible light making zeolite an efficient photocatalyst for degradation of dyes.

2.0 Literature Review

Zeolites are crystalline microporous aluminosilicate minerals characterized by their regular framework structure and high surface area. These materials are perfect for use including adsorption, ions exchange, and catalytic because of their three-dimensional network of linked channels and cages. The open framework and diverse composition of zeolites provide them special exchange of cations, ion specificity, adhesion, and molecular sieving capabilities(33). Zeolites are beneficial in many agricultural and environmental applications because of these characteristics. In addition to being employed as slow-release fertilizers, plant growth media, and animal feed additives, natural zeolites have been used for the sorption and removal of organic compounds, radioactive substances, heavy metals, and ammonium from rivers and lakes, soils, and sediments(34).

Numerous artificial zeolite species have also been created in labs for commercial ion-sieving or catalytic uses, numbering in the hundreds to thousands. Like quartz (SiO_2), zeolites belong to the class of silicate rocks known as tectosilicates. These minerals are made up of silica (SiO_4) tetrahedra with all four of their oxygens with neighbors in a 3-D construction. The elements in the tectosilicate structure(35). Zeolites come in 253 distinct framework types and can be either naturally occurring or artificially produced. These aluminosilicates were used more frequently, particularly after the Food and Drug Administration (FDA, 2020) declared them "safe for human consumption" and the International Agency for Research on Cancer (IARC, 1997) declared them "non-toxic." Since erionite has an elevated iron level and is fibrous, it is the only kind that is regarded as carcinogenic(36). Different scientists synthesized zeolite used for the degradation of dyes.

The dye photo-catalytic removal was studied by M. Mansouri et al. utilizing zirconia nano catalysts, zeolite (Ze), ZrO_2-Ze in varying ratios, and optimized ZrO_2-Ze doped with urea, copper oxide, and cerium oxide. Under ideal circumstances, methyl orange (MO) dye removal (100%) was accomplished in 80 minutes under UV radiation(37).

Jaikishan Swain and colleagues developed $BaTiO_3$ ZIF-8 nanocomposites for the photocatalytic degradation of methylene blue (MB) under solar radiation by loading BaTiO3 nanoparticles into a Zeolitic Imidazolate Framework (ZIF-8). ZIF-8 has been synthesized in the presence of BaTiO3 to enable ZIF-8 to grow on the surface of $BaTiO_3$ and to promote the seamless transfer of charge carriers between the two materials. The composition with the greatest photocatalytic

activity is 25 weight percent $BaTiO_3$ ZIF-8. Under sun radiation, this composite effectively breaks down 93% of the MB dye in 180 minutes and totally breaks down the Congo Red dye in 75 minutes(38).

Using various aluminum sources, Mostafa Y. Nassar et al. reported on adjusting the shape and crystallite size of the hydrothermally produced zeolite nanostructures. The study found that precursors of aluminum metal, aluminum isoprenoid, and alumina created analcime nanoparticles, but precursors of aluminum sulfate and aluminum chloride produced non-crystalline forms. A combination of analcime and nacrite phases, with a crystallite size of around 77.95 nm, was produced by the sodium aluminate precursor, however. According to the results, the zeolite nanostructures as generated might be employed to remove methylene blue (MB) dye from aqueous solutions by acting as both adsorbents and photocatalysts at the same time. Fascinatingly, in the presence of UV light, zeolite photocatalyst made with aluminum isoprenoid destroyed the MB dye 85% and 100% in 180 and 110 minutes(39).

By employing the sol-gel process to disperse TiO_2 over the ZSM-5 zeolite's surface, calcining it at varying temperatures, and then modifying it with varying amounts of nickel nanoparticle precipitation, Khadije Badvi et al. were able to effectively create nano photocatalysts. To compare the produced nanocomposites with hydrogen peroxide-assisted photocatalytic degradation, catalytic hydrogen peroxide oxidation, and adsorption processes for dye removal from aqueous solution, the photocatalytic activity for the degradation of methylene blue dye was examined under UV light irradiation. The nano photocatalyst containing 0.5% nickel nanoparticles and a calcination temperature of 600 °C had the best UV photocatalytic degradation efficiency of around 99.80%(40).

With the use of supercritical pretreatment, Li You-ji et al. created nanocrystalline TiO_2-zeolite surface (TZS) composites using a unique sol-gel approach. The behavior of TZS in the catalytic degradation of Rhodamine B (RhB) dye under UV light was investigated in relation to the starting concentration of RhB, light intensity, irradiation period, TiO_2 coating ratio of TZS and its concentration in solution, and pH values in solution. For the quickest rate of RhB photocatalytic degradation, the ideal parameters were a concentration of 2 mg L^{-1} at pH 10, 32 mW cm^{-2} of light, and a catalyst content of 6 g L^{-1}(41).

Using rusty iron waste and natural zeolite, Fatma Mohamed et al. created Fe_2O_3 and Fe_2O_3-zeolite nanopowders by chemical precipitation. The chemical composition, structural

characteristics, and optical properties are investigated utilizing a variety of approaches in addition to the nanomorphologies. Comparing the Fe_2O_3-zeolite photocatalyst to Fe_2O_3, the former demonstrated smaller sizes and greater absorption of visible light. Fe_2O_3 and Fe_2O_3-zeolite are both employed as photocatalysts for the photodegradation of methylene blue (MB) in the presence of sunlight. The maximum performance to date for Fe_2O_3-based photocatalysts is 75 mg of Fe_2O_3-zeolite under visible light after 30 s, which fully photocatalyzes the breakdown of MB dye (10 mg/L)(42).

A new ternary composite $CdS/TiO_2/CeO_2$ and its zeolite-support was created by Mohammedsani Mahamud et al. and studied by XRD, SEM, UV-Vis DRS, and PL spectroscopy. An aqueous solution of Methylene Blue (MB) dye and a solution of actual sewage samples were used to examine the photocatalytic performance of the produced nanocomposites.In comparison to the naked $CdS/TiO_2/CeO_2$ binary and single counter components, the zeolite-supported composite exhibited better photocatalytic activity. Based on the adjusted parameters, the supported composite performed noticeably better on the discolouration of MB (99.9%) than the actual sewage sample solution (78.7%)(43).

Using ZSM-5 zeolite-doped polyaniline composites, Veena Sodha et al. demonstrated the photocatalytic degradation of methylene blue. In situ oxidative polymerization is a straightforward method used to create ZSM-5-based polyaniline (PANI) composites. PAZe-1, PAZe-5, and PAZe-10 are the labels given to the samples, which were synthesized using various weight ratios of ZSM-5. By tracking the deterioration of methylene blue in the presence of visible light, the photocatalytic performance of polyaniline, ZSM-5, and their composites was evaluated. PAZe-1 had the greatest performance when comparing the photocatalytic efficiencies of various composites, with a 99.9% degradation efficiency after 210 minutes of irradiation. In contrast, PANI, PAZe-5, PAZe-10, and ZSM-5 displayed removal efficiencies of 38%, 82%, 71%, and 99%, respectively(44).

2.1 Zeolite Interaction with Metals

There is a noticeable drop in the energy band gap from 4.84 eV to 4.33 eV when Zn2+ centers of metal in mixed metal are replaced with Cd2+ ions. With a higher ratio of Cd ions, the band gap energy decrease is shown, suggesting that the band gap can be efficiently modulated by adding other metals. This correction appears to result from modifications to Cd's electronic structures that affect the conductance energy. Compared to basic element doping, this method works better at tuning the band gap. Three different

scales of 0.8, 0.9, and 1.0 were used to analyze the van der Waals radii in order to determine resolution(45).

Examining the effects of adding mixed metals to metal-organic structures (MOFs) provides important insight into how different metal distributions affect chemical bonding, electronic properties, particularly the arrangement of net nuclear charges, and their interactions with molecules. In mixed-metal ZIFs, increasing the Zn^{2+} content causes the lattice parameters to decrease and affects the bond lengths between the metals and linkers. The nature of the bond among the metal and organic binder can also be understood by identifying the chemical bonding inside mixed metal.

The Zn–N bond is found to have more bond characteristic than the Cd–N bond, which suggests that the two bonds have different strengths. Furthermore, a thorough understanding of how different CO_2 placements affect binding energy was offered by the investigation of CO_2 interactions with mixed metals in various positions. Along with the ensuing consequences for the removal of CO2, the work demonstrated the relationship between the composition of mixed metals and their electrical characteristics(46).

By altering the solvothermal conditions, two sets of mixed-metal zeolitic imidazolate frameworks (ZIF-62) were created, combining cobalt and zinc. The shape of the final ZIF crystals was notably sensitive to the synthesis conditions. One set of ZIF crystals followed the standard ZIF-62 pattern, and the other set displayed a combination of the standard structure and an unknown one. The addition of cobalt to replace zinc in the composition caused a minor deviation from linear tendencies in the conventional sequence with regard to the Tm (melting temperature) and Tg (glass temperature). On the other hand, the recently released series shows a more noticeable negative departure.

These deviations from a linear trend, which are negative, indicate the influence of mixed metal nodes in bimetallic ZIF-62 systems. Because of their different electronic structures and structural incompatibilities, Co^{2+} and Zn^{2+} exhibit this effect. In contrast to the normal series' homogeneous phase, the novel series exhibits a mix of cobalt- and zinc-enriched phases. Calculations using density functional theory predict that replacing Zn with Co will increase the bulk elasticity of ZIF crystals. By changing the metal node and adjusting the synthesis conditions, this study highlights the possibility of customizing the mechanical properties, melting properties, and structure of ZIFs. Interestingly, higher Tg/Tm ratios (from 0.77 to 0.84) in both sets of ZIFs

indicate improved glass-forming properties. When compared to the most skilled glass-forming materials, this puts them in a higher range(47).

We concentrated on examining Zn (2-methylimidazolate)2 and Zn(2-fluoroimidazolate)2. While the fluoro group allowed for the selection of up to three advantageous framework types, the methyl group was shown to provide an important level of polymorphism to the system. The ligand-to-ligand interactions were examined as crucial elements influencing the direction of particular network topologies(48). The structures are widely used in cutting-edge energy fields such as energy collection, retention, and catalysis. The present study is concerned with evaluating the band gaps of both unmodified and doped ZIF-8. Doping is the process of adding noble and different transition metals, like copper (Cu), titanium (Ti), and manganese (Mn). This investigation may provide a viable way to improve electrical characteristics by adding dopants that aren't dependent on noble metals (9).

Because of their large specific surface area and distinct pore patterns, metal-organic frameworks (MOFs), like ZIF-8, are extremely porous materials with extensive applications in a variety of fields. Creating composites by combining metal oxide and MOF is one method to improve the physical properties of ZIF-8. ZIF-8 and ZIF-8/Al2O3 were successfully synthesized using solvothermal technique, with aluminum variants of 19%, 38%, and 76%. The ZIF-8/Al2O3 composites were characterized by means of N2 physisorption, FTIR, SEM, and XRD. The ZIF-8 crystals' morphology showed a cubic form. In contrast to pure ZIF-8, the ZIF-8/Al2O3 composites showed different forms. A Zn-N signal at 420 cm-1 in the FTIR measurement showed the metal-organic ligand connection(49).

Vapor-assisted conversion was used to produce ZIF-8 nanoparticles, with n-heptane, methanol, and DMF serving as solvents. XRD, TGA, nitrogen (N2) sorption, FTIR, and SEM were among the methods used in the thorough analysis of these ZIF-8 samples. The diameters of the particles fall into three different ranges: 10–20 μm, 60–90 μm, and 30–50 μm. To the best of our knowledge, this is the first instance of ZIF-8 synthesis employing nonpolar n-heptane in a vapor-assisted conversion procedure. Comparing this method to traditional solvothermal techniques, the solvent consumption was significantly reduced as just 0.5 mL of solvent was required for ZIF-8 production(50).

An innovative Zn and Co-based zeolitic imidazolate framework (ZIF) structure has been successfully produced at ambient temperature using a simple and basic technique. To verify the

formation of a sodalite (SOD) cage-like structure, characterization methods including SEM, TEM-EDX, single-crystal XRD, and ICP analysis were employed. The high nano-crystallinity and porosity of the Zn/Co-ZIF are two notable features that contribute to its substantial surface area. Altering the Co and Zn ratios has enhanced the Zn/Co zeolitic imidazolate framework's physical and chemical capabilities, surpassing those of the individual metal architecture (ZIF-8 and ZIF-67). After that, the Zn/Co-ZIF was studied in two different environments: gas adsorption and catalysis. Hydrolytic stability tests were performed to further illustrate the enhanced stability of Zn/Co-ZIF(51).

Guidelines for improving the electrical conductivity in zeolitic imidazolate frameworks are developed using electronic structure simulations. Co2+-based frameworks were previously found to have electrical resistivity values that were roughly 1000 times lower than those of Zn2+-based materials. Furthermore, the control of framework electrical conductivity is made possible by the choice of ligand molecules. This changeable electrical conductivity is explained by analyzing the nature of the conduction band edge using density functional theory calculations.

This research shows increased hybridization and band characteristic expansion in the Co2+ centered structures. These improvements in the methyl imidazolate structures are associated with better frontier orbital alignment between the ligand and metal. A path for the methodical production of robust framework materials suited for electronic applications is provided by the intrinsic flexibility and the previously described straightforward synthesis procedure. By laying out these guidelines, we prepare the ground for the upcoming development of robust, electrically conductive zeolitic imidazolate frameworks(52).

2.2 Role of Zinc Oxide in Cosmetics & Sunscreen Products

UV rays are a small fraction of the sunlight but they carry some dangers to the skin, which includes getting sunburned, getting aged skin, and skin cancer. Thus, sunscreens are heard to be one of the most necessary cosmetics to counteract these drastic effects. Sunscreens are classified into two main categories: It includes; Chemical and physical. Physical sunscreens, and more especially, titanium dioxide and zinc oxide, which are stop gap measures in this discourse, work by two principal processes namely reflection and scattering. While chemical sunscreens cause the skin to absorb the UV radiation, physical sunscreens physically sit upon the skin and bounce the UV rays off from the skin. This two-pronged strategy of physical closure makes physical sunscreens very useful in protecting the skin against injurious UV radiation. Damaging effects of

ultraviolet radiation include erythema, premature aging and skin cancer (53).

Also, the sunscreens based on zinc oxide are non-allergenic, non-irritating and non-comedogenic; they therefore suit persons with sensitive or highly irritated skin. Physical sunscreens contain a major ingredient of zinc oxide that acts as reflected and scattered UV shielding agents (54). Also, it is known to create a soothing effect on irritated skin: it brings down inflammation and redness. Zinc oxide works nicely to completely heal and clear oily skin with dry or acne-prone skin (55). Furthermore, its ability to absorb excess oil makes it a popular choice in cosmetic formulations designed for individuals with oily or acne-prone skin.

The various functional benefits of zinc oxide make it a very versatile, integral part of sunscreens and skin care products, ensuring protection against UV-induced skin damage in the best possible way as well as promoting the health and comfort of skin. Due to the number of functional applications, zinc oxide remains a widely used and an essential component of sunscreens and skin care products in preventing UV modulated skin damage and helping to improve skin health and comfort (56).

2.3 Role of Zinc oxide in Medicine

Zinc oxide (ZnO), having unique semiconducting, optical, and piezoelectric properties, properties which could present a wide variety of nanostructures, has been investigated for as many varied applications (57). The use of zinc oxide nanoparticles (ZnO NPs) has increased in a number of commercial products, including paint, rubber, coatings, and cosmetics.Because of their exceptional biocompatibility, affordability, and low toxicity, zinc oxide nanoparticles (ZnO NPs) have been one of the most widely employed metal oxide NPs in biological applications over the last 20 years.Because of their strong propensity to liberate zinc ions, cause excessive reactive oxygen species (ROS) generation, and promote cell apoptosis, ZnO NPs have shown great promise in biomedicine, particularly in the antibacterial and anticancer domains.(58, 59). Antibacterial properties are achieved in ZnO nanoparticle suspensions against a diverse range of microorganisms (60). Furthermore, it is widely known that zinc maintains the structural integrity of insulin. Thus, ZnO NPs have also been successfully created for the treatment of diabetes. Zinc oxide nanoparticles have antibacterial qualities and a variety of toxicity mechanisms.Additionally, ZnO NPs have outstanding luminous qualities, making them a leading contender for bioimaging(61, 62).

Some of the features of ZnO that are promising for using in therapeutic purpose in medicine are

the following. These include; the antibacterial, antifungal as well as the anticancer ability of Zinc Oxide nanoparticles. For reactivity, the generation of ROS by ZnO NPs can damage the membrane and DNA of bacterial cells. ZnO NPs are proved to interrupt bacteria's metabolism and inhibit new biofilm formation. Among the very best qualities of ZnO for therapeutic application are in medicine, antibacterial, antifungal, and anticancer activity of the Zinc Oxide nanoparticles. This is because this bacterium cell membrane and DNA damage done by ROS generated by ZnO NPs will interfere with the metabolism of bacteria and prevent the further formation of new biofilm (58).

Antifungal activity of the ZnO NPs was also confirmed against a wide variety of pathogenic fungi. The mechanisms of activity are the disturbance of the integrity of the cell wall and inhibition of the fungal enzymes, with the generation of ROS that damage the fungal cells. The use of ZnO NPs has also been done in fungal skin, nail, and mucous membrane infections. ZnO nanoparticles are created and examined for their antiseptic properties and toxicity mechanism (63).

Anti-cancer activities of ZnO NPs have attracted enormous attention. ZnO NPs have been reported to induce apoptosis in cancer cells by elevation of ROS, mitochondrial dysfunction, and activation of cell death pathways. The applications of ZnO NPs have been investigated against several types of cancer, like breast cancer, lung cancer, and prostate cancer. Zinc oxide nanoparticles show technological advances and prospects for cancer therapy (64).

Other than antimicrobial and anticancer activities, ZnO NPs possess activity in areas such as wound healing and drug delivery. ZnO NPs have been applied to wound dressings and ointments, where wound healing is helped through downregulation of inflammation and reduction of infection via a germicidal effect, as well as the stimulation of the cells at the wound to regenerate. ZnO NPs have been used in developing a drug delivery device because they can encapsulate and release drugs in a controlled manner. ZnO nanoparticles are a versatile agent that can perform multiple biomedical functions (65).

2.4 Zinc Oxide Role in Textile & Ceramics

Currently, zinc oxide nanoparticles (ZnO) are considered as one of the most effective antimicrobial agents to be used in textile processes since they can kill bacteria and prevent the

growth of molds on fabrics (57). Thus, there is additive value in this property for the use of the material in healthcare, sportswear or any product that may be sensitive to microbial contamination. ZnO nanoparticles can be built into the fiber during the manufacturing process or applied as a film to the fiber after manufacturing, so they can protect the fabrics lasting from odor, infection, and degradation (57).

In the case of ceramics, ZnO has an important function as a glaze material, improving the characteristics of the ceramic films. It is used to increase glazes' gloss, whiteness, and translucency as well as enhancing clearness and chemical resistance, and the overall resistant to abrasion and scratching. ZnO plays an important role in as a flux, which means that under high temperatures it reduces the melting point of glazes, making the flow more homogeneous and the end result – smoother (66).

Apart from the antimicrobial and glazing functions, ZnO has got other uses when it comes to the manufacturing of textiles and ceramics. In textile, zinc oxide nanoparticles are used to formulate value added finishes like UV protectants, self-cleaning, and durable moisture Management System. Ceramics use ZnO in the fabrication of piezoelectric materials that change mechanical stress to electrical signals for the creation of sensors, actuators and energy harvesting supplies (67).

The applicability of ZnO nanoparticles in Textile as well as ceramics sectors follows from various physicochemical characteristics such as; High surface area to volume ratio, photocatalytic properties and semiconducting nature (68). As such, ZnO nanoparticles are among the most useful materials to enhance the functionality, effectiveness, and durability of the textile and ceramic products that leads to the enhancement of both conventional and modern applications.

Additionally, zinc oxide is utilized in the electronics industry for its semiconductor properties, making it suitable for the fabrication of varistors, piezoelectric devices, sensors, and transparent conductive films. Its versatility and wide range of applications make zinc oxide a valuable material in various industrial sectors, contributing to advancements in technology, healthcare, and consumer products. ZnO nanoparticles have been investigated as both antimicrobial agents

and effective fertilizers, promoting plant growth and protecting against pathogens in agriculture (69).

2.5 Zinc Aluminum Silicate as Coating

Zinc aluminum silicate (ZAS) is a class of materials that got application over its uniqueness of properties as coatings in various industries. ZAS coatings are popular because of good thermal stability, chemical resistance, and mechanical strength. Such coatings are mainly applied to metal substrates as protection from corrosion, wear, and high-temperature oxidation. ZAS coatings are used in the aerospace industry to protect blades of turbines and other components of engines against the tough operating conditions in jet engines (70). The thermal stability and oxidation resistance of ZAS coatings help to extend the life of such components and, therefore, the engine efficiency.

In automotive engineering, the ZAS coating protects the exhaust system and other components from corrosion and high-temperature degradation (71). Chemical resistance provides protection against chemicals and the corrosion products, while thermal stability ensures the integrity of the coatings is retained at elevated temperatures. ZAS coatings are used in the chemical processing industry to protect reactors, pipes, and other equipment from corrosion and chemical attack (72). Thermal stability, chemical resistance, and mechanical strength are among the benefits of using zinc aluminum silicate (ZAS) coatings in protective applications (73). Due to the chemical resistance of ZAS coatings, they find favor in severe chemical environments where exposure to acids, alkalis, and other corrosive substances is encountered. Apart from protection, ZAS coatings can add value to the aesthetic appeal of products. ZAS can be formulated in different colors and finishes to satisfy specific design needs.

Zinc-rich coatings, pure zinc or Zn/Al alloy metallic coatings, and zinc-base coverings with a top covering on the aluminum alloy 5086 were among the types of zinc base coatings with galvanic protective capabilities whose blistering behavior and processes were investigated in seawater immersion. After ten months in the water, the zinc-rich coatings were largely immune to the blistering, but the pure zinc and Zn/Al alloy coatings showed noticeable blistering on the whole coating surface. The zinc-rich coatings did not provide the alloy 5086 with adequate galvanic protection, despite the metallic coatings. The presence of zinc corrosion products in metallic

coatings is the primary cause of blistering.Under conditions of exposure to seawater, the behavior and mechanisms of the creation of various zinc-based coating types were examined. The formation of zinc saving products in the paint is the main cause of piping in metallic coatings(74).

Atoms of silicon, aluminum, and zinc are grouped in a silicate structure to form zinc aluminum silicates. Researchers have looked into using zinc aluminum silicate (ZAS) coatings to enhance the thermal barrier properties of materials in high-temperature applications like the energy and aerospace sectors(75). Because of these compounds' special qualities, they are used in a wide range of sectors. The manufacture of glass and ceramics is one typical use for zinc aluminum silicates. These substances are used as ingredients in glass formulations and ceramic glazes to add particular qualities including hue, transparency, and thermal stability. Because of their non-toxicity and immunity to corrosion, zinc aluminum silicates (ZAS) have been investigated as an environmentally acceptable covering(76).

Also, zinc aluminum silicates are used as fillers and reinforcements in polymer matrix composites; these enhance the mechanical properties of the resultant composites such as high strength, heat stability, and fire resistance. In cosmetics and personal care products especially, those belong to rinse-off products, zinc aluminum silicates are used as bulking agents, opacifiers, and absorbents in products like powders, creams and lotions. In addition, these compounds have uses in the field of drug formulation as diluents in tableting of medicines and in controlled-release medications systems. In addition, zinc aluminum silicates are used in industrial applications such as, water softening and clarification, catalyst supports, and in soil stabilizers. Further applications for zinc aluminum silicates include: the use as mineral filler and reinforcement in polymers; matrix composite in industrial applications, for example, water softening and clarification, catalyst supports; and the soil stabilizer (77).

2.6 Factors Affecting Photocatalytic Performance of Zn-Doped Zeolites

The photocatalytic performance of Zn-doped zeolites is impacted by several things: the type of zeolite framework, the concentration of zinc doping, synthesis method, and calcination conditions.

The type of zeolite framework plays a crucial part in the photocatalytic activity of Zn-doped zeolites. The different zeolite frameworks have different pore sizes, surface areas, and chemical compositions, and hence influence the sorption and diffusion of reactants and products. For example, it is more plausible that a larger pore size and higher surface area of zeolites would

enhance their photocatalytic activity because such a structure would give more surface area for the adsorption of reactants and will provide easy access to the active site. Zn-doped zeolites exhibit photocatalytic activity strongly dependent on the type of zooplastic rock framework, which affects their pore size, surface area, and chemical composition (78).

Zinc doping concentration also has a significant impact on zeolites' photocatalytic activity.

A required amount of zinc doping is effective in increasing the photocatalytic activity, but an over doping quantity forms zinc oxide clusters that might act as recombination centers for photogenerated charge carriers, diminishing the overall efficiency of the photocatalytic process (79). Thus, it is important to optimize the zinc doping concentration to get the best possible photocatalytic performance. The photocatalytic activity of the prepared Zn-doped zeolites can also be affected by the type of synthesis method. Zinc ions' distribution within the zeolite framework, particle size and morphology, as well as impurities or defects, can all be determined by how the method of synthesis is used; these factors can affect photocatalysis (80). As such, various synthesis methods may lead to the possible difference in the distribution of zinc ions in the zeolite framework, particle size and morphology of the zeolites, and the presence of impurities or defects. All these factors will affect light absorption properties, the effectiveness of separation of charges, and hence, zeolites' overall photo catalytic efficiency. Under these lights, judiciously selecting and optimizing the synthesis method is important to attain Zn-doped zeolites with targeted properties.

The photo catalytic activity of Zn-doped zeolites may also be influenced by calcination conditions, mainly temperature and time duration. The characteristics of zinc ion fixation, and the ZnO clusters' formation depend on temperature and time during calcination, which determines the photo catalytic properties of zirconium-doped zeolites (81). Calcination is the process of heating treatment applied to zeolites containing impurities to remove these impurities, to enhance the crystallinity, and to activate the zeolites. Nevertheless, the high temperature of calcination or an extended time of calcination may cause lost zinc ions from the zeolite framework or aggregation of ZnO cluster, which will deteriorate the photo catalytic activity. Consequently, optimization of calcination conditions is critical to maintain the targeted characteristics of Zn-doped zeolites. To summarize, The Zn-doped zeolites' photo catalytic abilities is controlled by complete structure frame reasons, zinc concentration, synthesis approach, and

calcination method. These factors, along with the optimization of their performance, are essential to achieve an effective and sustainable Zn-doped zeolite photocatalyst for environmental and energy applications (82).

2.7 Synthesis of Zn-doped Zeolites

During the synthesis of Zn-doped zeolites, the zinc ions are incorporated into the zeolite framework. The ion exchange process is frequently used to incorporate zinc ions into pre-synthetic zeolites, which are typically in the form of sodium (83). Methods of this nature count ion exchange, impregnation, and direct synthesis among the techniques available. The zeolites are pre-synthesized in this method as an immature zeolite (in the sodium form) and sodium ions are exchanged with zinc ions from a zinc salt solution. In the incipient wetness impregnation method, zeolite was impregnated in a zinc salt solution, followed by drying, and then calcination for the zeolite to keep the zinc ions in the framework (84). Here, for the direct synthesis method, the process of zeolite synthesis, such as adding zinc ions into the synthesis gel, is used. Therefore, the type of synthesis route also affects the distribution and cooperation of Zn in the zeolite network which could influence the photo catalytic activity.

2.8 Characterization of Zn-doped Zeolites

Characterization of Zn-doped zeolites is very much necessary for their structural, chemical, and optical properties that also play a very important role in photocatalytic activity. To this aim, many techniques are applied, such as XRD, FTIR, SEM, TEM, and XPS. X-ray diffraction furnishes information regarding the crystallinity and phase purity of the zeolite, while FTIR affirms the functional groups present and the interaction between zinc ions and the zeolite framework. SEM and XPS provides information on the chemical composition of the zinc ions' surface and their oxidation state, whereas TEM provides information about the zeolites' shape and particle size. UV-Vis diffuse reflectance spectroscopy is the primary method for measuring the ban-dgap energy of Zn-doped zeolites, which is crucial in determining their ability to absorb light for photo catalytic reactions (85). The local location and coordination of zinc ions within the zeolite framework can be observed through NMR spectroscopy, which also provides information about their catalytic activity (86).

2.9 Photo catalytic Applications of Zn-doped Zeolites

Zn-doped zeolite can find prospective photocatalytic activity in degradation of organic pollutants, water splitting for hydrogen production, and carbon dioxide reduction. Therefore, enhanced photocatalytic activity of Zn-doped zeolites was ascribed to high light absorption, effective charge separation, and an increased surface reactivity toward zinc ions' introduction (87). When exposed to UV or visible light, zinc-doped zeolites effectively break down organic contaminants, including most organic colors, insecticides, and medications. The Zn-doped zeolites' electrons and holes produced by photosynthesis can combine oxygen and water molecules to create reactive oxygen species, like superoxide and hydroxyl radicals, which can oxidize and break down organic contaminants. Photocatalysis of organic pollutants, such as dyes, pesticides and pharmaceuticals using zeolites doped with Zn, has been shown to be promising under UV or visible light irradiation (88). The TiO_2-zeolites photocatalysts produced by solvothermal and impregnation methods were compared by Naruemon Setagaya et al. As demonstrated by their unique surface areas, microstructures, and mineralogical compositions, the solvothermal and impregnation methods' zeolites exhibited a striking resemblance in the integration of TiO_2 in the form of transparent titanium solution. The TiO_2-zeolites photocatalysts generated by the solvothermal approach had an adsorption and degradation efficiency of 97.32%, which was marginally less than the impregnation method's 99.43%(89). A new zeolite clay based on nanocomposite technology was effectively created by Redouane Haounati et al. utilizing a cost-effective and environmentally responsible method. When exposed to visible light, the resulting nanocomposite demonstrated significant photocatalytic effectiveness in removing the dangerous Rhodamine B dye from aqueous solution, with a clearance rate of almost 100%. Because of the improved adsorption ability onto the Zeo@Ag_2O nanocomposite surface and the high effective separation of photogenerated electron–hole pairs, the increased photocatalytic activity may be the result(90).

TiO_2-zeolite photocatalyst was created by Sri Wardhan et al. by impregnating acid-activated natural zeolite with TiO_2. TiO_2 is responsible for the anatase type, while mordenite and clinoptilolite types prevail in the natural zeolite employed in this work, according to the XRD data.The best results are obtained at pH 11 after 50 minutes of UV irradiation, with a 98.25% degradation amount. Remarkably, there is a 77.9% reduction in the chemical oxygen demand (COD) in the deteriorated MB aqueous solution, indicating an increase in the quality of the water(91). The ternary system g-C_3N_4/ZnO/CeO_2 and its unique zeolite-supported

nanocomposite were synthesized by Shimelis Girma et al. and studied using XRD, UV–Vis DRS, SEM, and PL equipment. After investigation, the zeolite-supported g-C_3N_4/ZnO/CeO_2 nanocomposite's photodegradation efficiency for MB dye and textile processing effluent was determined to be 95.2% and 72.77%, respectively. The impact of working factors, including pH, beginning dye quantity, and catalyst dosage, on MB dye photodegradation was examined using a zeolite-supported (STZ) composite. Under ideal working conditions, the bare ternary system's photodegradation efficiencies and that of its zeolite-supported equivalent were found to be 81.74 and 95.89%, respectively(92). A novel CuO nanoparticle (CuO NPs) coated Zeolitic Imidazolate Frameworks (ZIF-8) photocatalyst with a better catalytic activity for dye degradation was synthesized and characterized by Anindita Chakraborty et al. To create ZIF-8 cubes (about 80 nm), a sol-gel technique was used. CuO nanoparticles were grown and nucleated in-situ on the cubic ZIF-8 surfaces.It was decided to use the as-synthesised material as a photocatalyst to break down the rhodamine 6G (Rh6G) dye. The ZIF-8 photocatalyst, which was deposited using ultra-small colloidal CuO nanoparticles (~5 nm), demonstrated effective photocatalytic activity for Rh6G degradation when exposed to sunlight. The best photocatalytic activity for dye degradation is shown by a nanocomposite that contains 5 weight percent CuO nanoparticles(93).

Using zeolite-supported TiO_2 and Fe-doped TiO_2/zeolite photocatalysts, Ghania Foura et al. sought to enhance the microporous support's adsorption capabilities against polluting dyes and the photocatalytic efficacy of TiO_2 in treating the adsorbed organics. The photocatalytic degradation of methylene blue, or MB, over 10 weight percent TiO_2/HY under UV light at 254 nm was best performed by the TiO_2/HY zeolite catalyst. A catalyst known as Fe-TiO_2/HY was produced by adding Fe species to the synthesis mixture. The degradation of the model dye was remarkably effective due to the combination of Fe doping, efficient titanium dioxide dispersion, and sufficient zeolite. A complete elimination of MB (>98%) was accomplished after 60 minutes under extremely mild circumstances over a 10 weight percent Fe-doped TiO_2/HY catalyst(93). In order to photo-catalytically degrade Eriochrome Black T (EBT) and Methyl Orange (MO) under UV light irradiation, Maryam Karimi-Shamsabadi et al. employed photo-catalyst NiO-ZnO doped onto nano zeolite X (NZX) with a p-n heterojunction semiconductor structure. For the degradation of (EBT) and (MO), the composites showed noticeably increased photo-degradation activity. Mixed p-type NiO and n-type ZnO oxides added to NZX have been shown to have a synergistic impact on the photo-degradation process(94).

Thorough characterization and photocatalytic performance tests of the Zn-doped zeolites will provide a comprehensive understanding of the structure-activity relationship and their practical application in wastewater treatment. The results obtained from this study are thus expected to lead to the creation of photocatalytic materials that are effective, stable, and sustainable for environmental remediation.

CHAPTER-3EXPERIMENTAL

3.0 METHODOLOGY

3.1Materials and chemicals

Forerunner of Silica**,** Zinc acetate**,** Ethanol, $ZnSO_4.7H_2O$, citric acid, ammonia, $NaNO_3$, H_2SO_4, $KMnO_4$, H_2O_2, HCl, Sodium hydroxide, polyethylene glycol (PEG), aluminum chloride hexahydrate, and Deionized water.

3.2 Synthesis of Zinc Oxide Nanoparticles (ZnO NPs)

A suitable quantity of $ZnSO_4.7H_2O$ (147.33mg) was dissolved in 10 mL of distilled water for the preparation of ZnO. The solution has pH 5 currently. After that citric acid was added and after 20 minutes' pH was reached at 3. Then solution was continuously stirred for 1 hour. By adding liquid ammonia (0.2M) solution, the combination was kept at a pH of 8.0. Repeatedly used distilled water to wash the material. To form a gel, the fluid was then dried at 80°C. Following a grinding of the powder, it was calcined for 4 hours at 400°C.

3.3 Synthesis of Zinc doped Zeolite (Zn-Zeolite)

Using the co-precipitation approach, zinc aluminosilicate ($ZnO.Al_2O_3.Si_{10}O_{20}$) was synthesized. To do this, 1 g of silica was added to 20 mL of water and swirled for 5 minutes. Sodium hydroxide (40 mg) and 48.8 mg of polyethylene glycol (PEG) were also added, and stirring was continued throughout. Zinc chloride (20 mg) was added to 5 mL of aqueous aluminum chloride hexahydrate (25 mmol). Every five minutes, at a feed rate of 0.02 milliliter min-1, 0.1 milliliter of the previously prepared solution was added to the silica solution. After that $ZnSO_4.7H_2O$ was added for doping of zinc with Zeolite. The mixture was constantly stirred, and then for 24 hours, the nanosize was achieved. The material was centrifuged for two minutes at 12,500 rpm, then dried overnight and washed with purified water until the pH of the filtrate was 7. The dry substance was calcined at 550 °C for four hours in a muffle furnace.

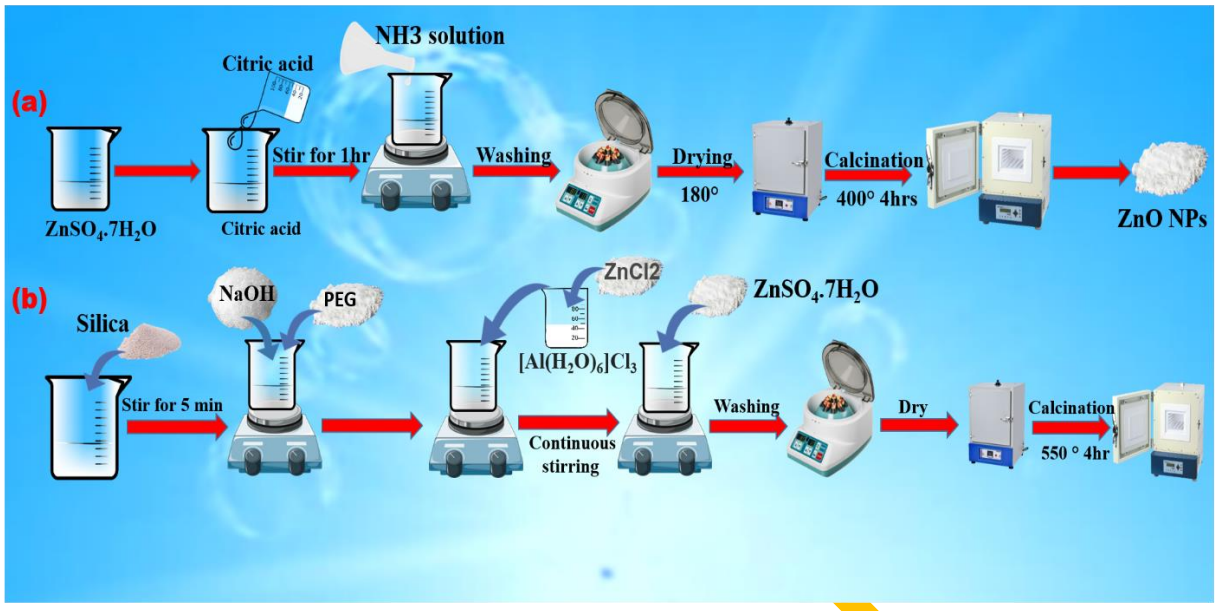

Figure 4 Synthesis of (a) ZnO NPs (b) Zn-doped Zeolite (Zn-Zeolite)

CHAPTER 4: RESULTS&DISCUSSION

4.0 Results & Discussion

4.1 FTIR analysis

The FT-IR spectra offer a comprehensive analysis of the functional groups and chemical bonds that are present in the samples in a range of 4000-400cm^{-1}.

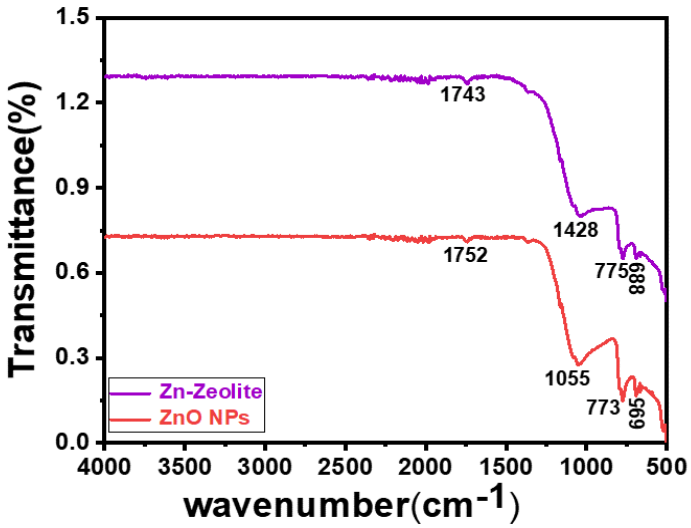

Figure 5: FTIR analysis of all prepared samples

Figure 5 shows the FTIR spectra of the ZnO nanoparticles (red curve), and the Zn doped zeolite composite (purple curve) whereby the discrete vibrational features can be observed to confirm the successful formation and interaction of the two constituents. The highest absorption at 1743cm^{-1} and 1752cm^{-1} are attributed to the C=O bands of the carbonyl groups or carboxyl groups, which could also be of the remaining organic species or adsorbed carbonates after synthesis(95). The band at 1428 cm^{-1} is linked with C-H bending or symmetric stretching of the carboxylate fragments, which shows the partial existence of organic fragments or adsorbed CO_2 in the atmosphere. The asymmetric zeolite studies the zeolite framework is associated with a strong band at 1055cm^{-1}, corresponding to the asymmetric stretching vibration of Si -O -Si bonds, and a slight change in this band as compared to pure zeolite indicates a structural modification and a strong interface reaction between ZnO and the zeolite framework(96). The characteristic bands at 773cm^{-1}, 698cm^{-1} and 655cm^{-1} are associated with vibrations of the framework and Zn -O -Si connections and this again indicates successful inclusion of ZnO into the zeolite structure.(97). A clear band in

the low frequency range at about 589cm^{-1}, the typical value of Zn -O stretch vibration, underpins the existence of ZnO nanoparticles in the composite system. The apparent change in the position and expansion of the zeolite related peaks with addition of ZnO are clear pointers of distortion of the lattice and chemical interaction and as such, it is possible to say that strong chemical bonding was formed as opposed to physical mixing. The latter are comparable with other reports in which ZnO stretching modes were found to be located in the 400-600cm^{-1} range, zeolite structural vibrations were recorded in the 1000-700cm^{-1} range, and a similar interaction between ZnO and zeolite was observed to take place.(98). In general, the FTIR seems to confirm the effective integration of ZnO to the zeolite structure leading to the formation of a stable hybrid structure consisting of increased interfacial bonding and structural stability, which is beneficial to catalytic and adsorption-based processes. (99).

4.2 XRD Analysis

Figure 6(a) and Figure 6(b) show the X-ray diffraction (XRD) patterns of ZnO and Zn doped zeolite, respectively. This is the characteristic diffraction peak of aluminum silicate in the Zn-zeolites sample that is represented by the (222) plane diffraction peak at 2θ of 12.6°. Other reflections with 2θ at 20.8° (100), 26.6° (011), 50.0° (112), 54.7° (022), 59.7° (121), and 68.0° (031) can be associated with the silicon dioxide (SiO_2) and hence they have the silicon dioxide (SiO_2) structure in the composite. A strong peak is observed at 2θ of 36.5° in the sample of ZnO in the (111) plane of ZnO which is consistent with PDF 03-065-0682. Moreover, there are some other peaks at 2θ of 39.42° and 42.40° in the Zn -zeolite composite that are indicated by the $ZnAl_2Si_{10}O_{24}$phase relative to PDF 00032145. These peaks indicate the crystal growth of the composite to form crystallographic growth in the hexagonal (200) and (201) planes indicating the hexagonal geometry of the ZnAl-SiO based phase. In the meantime, ZnO component of the composite displays strong diffraction peaks at 2θ 31.76°, 36.25°, 47.53°, 56.50°, 62.85° and 66.37° which may be indexed to (100) and (101), (102) (110), (103) and (200) respectively which are in line with the hexagonal wurtzite structure of ZnO (JCPDS card no. 01-079-2205) (98). This trend confirms that the ZnO does not change its crystalline hexagonal structure when incorporated in the zeolitic matrix.

The crystalline sizes of $ZnAl_2Si_{10}O_{24}$ nanocomposite calculated from Scherer's equation given below(100)

$$\textbf{Crystalline size}(\mathbf{D}) = \frac{\mathbf{k}\lambda}{\boldsymbol{\beta}\mathbf{COS}\boldsymbol{\theta}}$$

The X-ray wavelength is denoted by λ, the Bragg's angle by θ, the full width at half maximum (FWHM) by β, and the crystallite size by D. Scherer's constant, K, characterizes

the shape of the crystal(101). The average sizes were found to be 45 nm (ZnO) and 35.1nm (Zn-Zeolite).

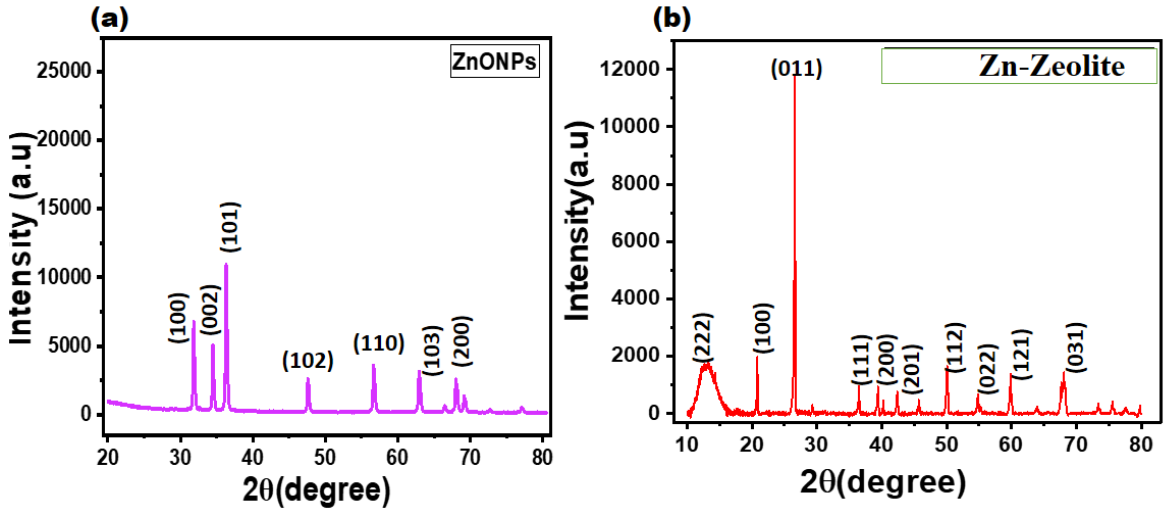

Figure 6: XRD pattern of (a) ZnO NPs (b) Zn-Zeolite

4.3 SEM Analysis

To determine the relationship between surface morphology and textual properties of ZnO and Zn-doped zeolite and their relation to photocatalytic activity, SEM and EDX analyses were conducted to provide an approximate image of surface morphology and textural characteristics of the samples, as shown in Figure 7. SEM image of low magnification (Fig. 7a) of the ZnO nanoparticles showed a very agglomerated morphology that assumed a rice shape characteristic of the ZnO nanostructures to cluster together because of high surface energy and van der Waals forces. Conversely, the high-resolution SEM image (Fig. 7b) indicated that small, almost spherical particles with irregular diameters were formed indicating that the nucleation and growth of ZnO crystallites had taken place during the synthesis. In case of Zn-zeolite composite, the low-magnification micrograph (Fig. 7c) had randomly dispersed flake-like structures, and the high-magnification micrograph (Fig. 7d) was characterized by heavy agglomeration of the nano-grains that enhance a high specific surface area and a small average particle size. This increased surface texture leads to increased light absorption and availability of active sites which explains the high photocatalytic activity of free Zn-zeolite as opposed to pure ZnO.

The micrographs of ZnO and Zn-zeolite were quantitatively analyzed with the Image J software which estimated the mean grain size to be 6.6 µm and 6.1 µm, respectively, which is

consistent with the crystal size measured with the XRD analysis, thus supporting structural consistency between the two methods. The elemental composition of ZnO was confirmed by the EDX spectrum of ZnO (Fig. 7e), which shows the homogenous populations of both zinc (Zn) and oxygen (O) elements, which confirmed the purity of the phase. At the same time, the EDX spectrogram of Zn-zeolite (Fig. 7f) showed that there was a presence of aluminum (Al), silicon (Si), carbon (C), oxygen (O) and zinc (Zn) in different percentages, which confirmed the effective addition of ZnO nanoparticles to the zeolite structure. Such morphological and compositional understandings ensure that the synergistic effect between ZnO and zeolite is used to improve the active surface area, adsorption capacity, and charge separation of the material resulting in better photocatalytic activity.

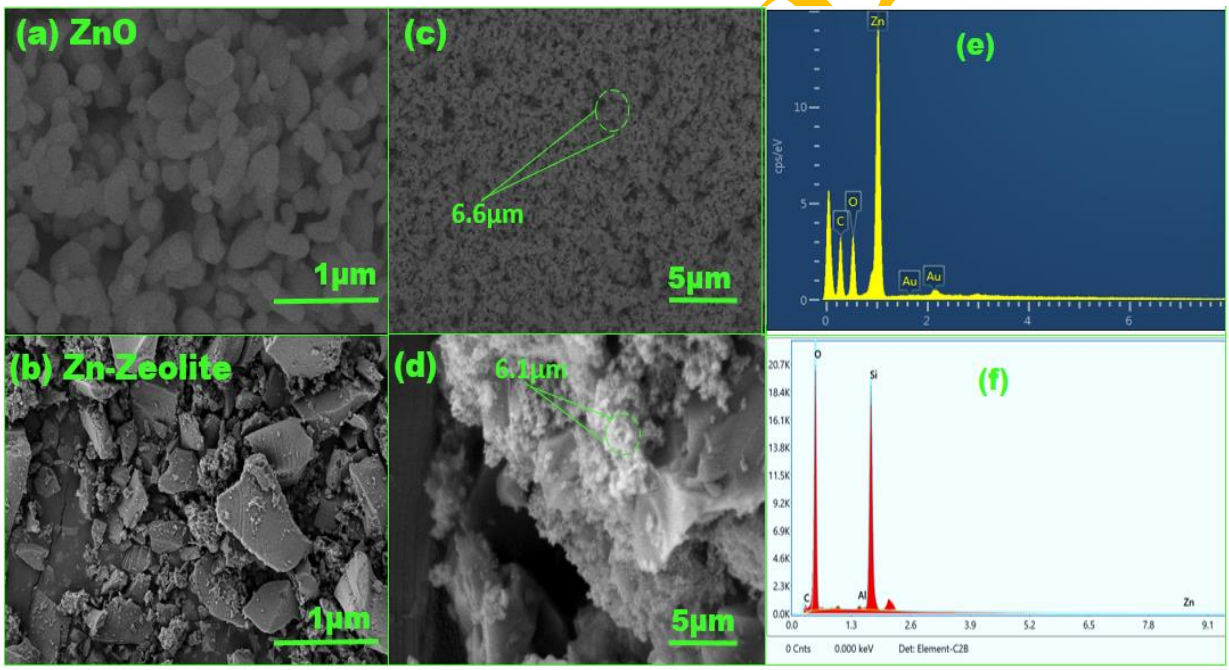

Figure 7: (a-b) SEM analysis of ZnO at different Resolution **(c-d)** SEM analysis of Zn-Zeolite at different Resolution **(e)** EDX analysis of ZnO (f) EDX analysis of Zn-Zeolite

4.4 Photo catalytic Activity

Methylene blue (MB), methyl orange (MO), and Congo red (CR) were used as model organic dyes pollutants to determine the performance of the synthesized catalysts in photo catalysis. Each dye in the form of a stock solution (100 ppm) was dissolved in 100mL of distilled water and photocatalytic experiments conducted by placing 100 mg of catalyst in 100mL of dye solution (10ppm). A magnetic stirring of the mixture in the dark (40 minutes) before being irradiated with light was done to achieve adsorption equilibrium between the dye molecules

and the catalyst surface. Photo degradation occurred under the visible light irradiation at a light source of 100W tungsten lamp which was used to activate the catalyst. A dropper was used to collect 5 mL aliquots at a given time, centrifuge the samples and determine the sample spectrophotometrically to keep track of the reduction of the absorbance intensity of the characteristic peaks of the various dyes. The results of the experiment as shown in Figure 8 indicated that the two catalysts had a reasonable photocatalytic activity with all the three dyes but the efficiency of the Zn -zeolite composite was highly higher than that of the pure ZnO nanoparticles. The synergistic effect of ZnO and zeolite support in improving the charge carrier separation, dye adsorption, and surface reactivity in the visible light can be attributed to this increased activity. The large surface area of the Zeolite and their porosity also promote the diffusion as well as reaction of the dye molecules with the reactive oxygen species formed on the ZnO surface thus enhancing the degradation kinetics.

The following relation was used to compute the removal efficiency percentage.

(Co-Ct)/Co = degradation efficiency (%)

where Ct is the dye's ultimate concentration following time t, and Co is its beginning concentration. In case of Methylene blue degradation efficiency was 96.3% in 135 minutes Methyl orange was 98% in 150 minutes and with Congo red was 99.4% in just 90 minutes.

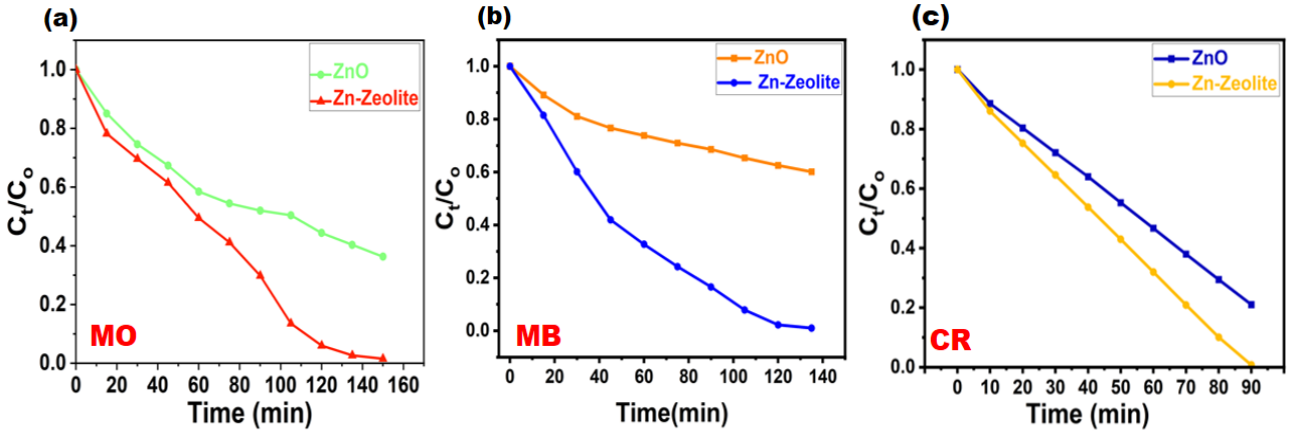

Figure 8. Photo degradation efficiency of ZnO and Zn-Zeolite for (a) MO (b) MB (c) CR

4.5 Photocatalytic Mechanism

The degradation mechanism of the dyes Methylene Blue (MB), Congo Red (CR) and Methyl Orange (MO) by Zn-doped zeolite as shown in the figure 9 can be described in detail due to

the photo-induced charge transfer and redox processes at the catalyst surface. When the Zn-doped zeolite semiconductor is exposed to visible radiation, electrons (e^-) are excited out of the valence band (VB) to the conduction band (CB), where they have sufficient energy to be emitted out of the particle and into the external environment. This process leads to the creation of photo generated electrons in the CB and holes (h^+) in the VB. Zn dopant is also important in lowering the bandgap energy of the zeolite framework and thus increasing the visible light absorption and reducing the rate of charge carrier's recombination by localized energy states at the conduction band edge. The photo generated electrons (e^-) in the conduction band are then transferred to the adsorbed oxygen (O_2) molecules on the catalyst surface, reducing them to superoxide radicals ($\bullet O_2^-$). These highly reactive oxygen species initiate the oxidative degradation of dye molecules such as MB, CR, and MO by breaking down their chromophore structures, ultimately converting them into non-toxic end products like CO_2 and H_2O. Simultaneously, the photo induced holes (h^+) in the valence band react with surface-adsorbed water (H_2O) or hydroxide ions (OH^-) to generate hydroxyl radicals ($\bullet OH$), which are known for their strong oxidative potential. These hydroxyl radicals further participate in the oxidation of dye molecules, attacking aromatic rings and heteroatoms, leading to complete mineralization of the organic pollutants.

The Zn ions incorporated within the zeolite framework enhance the separation of electron–hole pairs by acting as electron traps, thus prolonging the lifetime of charge carriers and improving photocatalytic efficiency. Moreover, the porous and high surface area structure of the zeolite facilitates effective adsorption of dye molecules, bringing them into close proximity with the reactive sites. The synergistic effect between Zn doping and the zeolite matrix therefore results in enhanced visible-light activity, superior charge transport, and improved photo stability. This integrated mechanism ensures efficient degradation of dyes like MB, CR, and MO, highlighting Zn-doped zeolite as a promising green photo catalyst for wastewater treatment and environmental remediation.

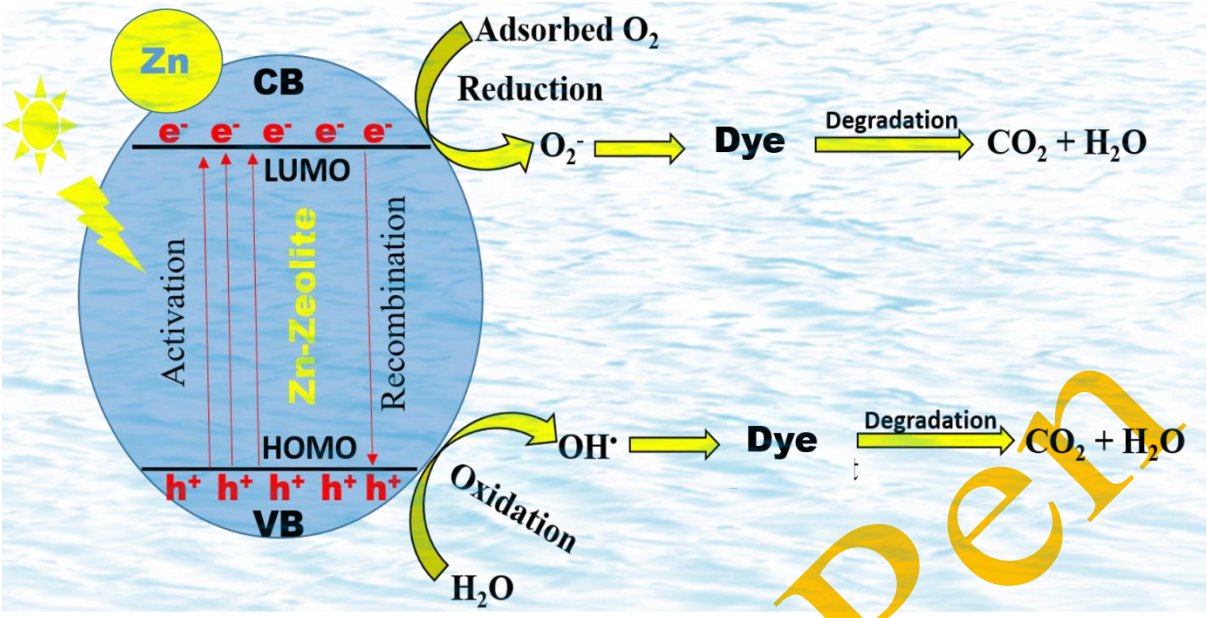

Figure 9 Photocatalytic Mechanism for degradation of dye catalyzed by Zn-Zeolite

4.6 Photo catalyst Stability and Reusability

The capacity of a photo catalyst to maintain both structural integrity and chemical stability during repeated catalytic cycles is one of the key properties of an efficient photo catalyst. This inherent stability makes the catalyst reusable on several occasions without it losing much activity. The present study has proposed a Zn-Zeolite photo catalyst and it underwent a reusability test to determine the stability of the material under continuous operational conditions. The used catalyst was collected by centrifugation and good washed with the deionized water to remove all leftover dye molecules or any intermediates adsorbed on the surface and then dried at 80^{o}C in an oven to re-expose the active surface to reuse. Experiments on photocatalytic degradation using individual dye solutions and a mixture of dyes were performed in a series of five cycles in succession as shown in Figure 10. The findings have shown that the efficiency of degradation of Zn -zeolite was almost constant, and a slight reduction of about 2 percent occurred after the fifth cycle. This slight drop in functionality suggests that the catalyst has a high level of photochemical stability, high structural integrity and photo corrosion resistance. This type of reusability proves that Zn -zeolite can be successfully utilized as a long-term wastewater treatment method, which corresponds to the results of other recent studies stating the significance of recyclability in the case of sustainable photo catalysts.

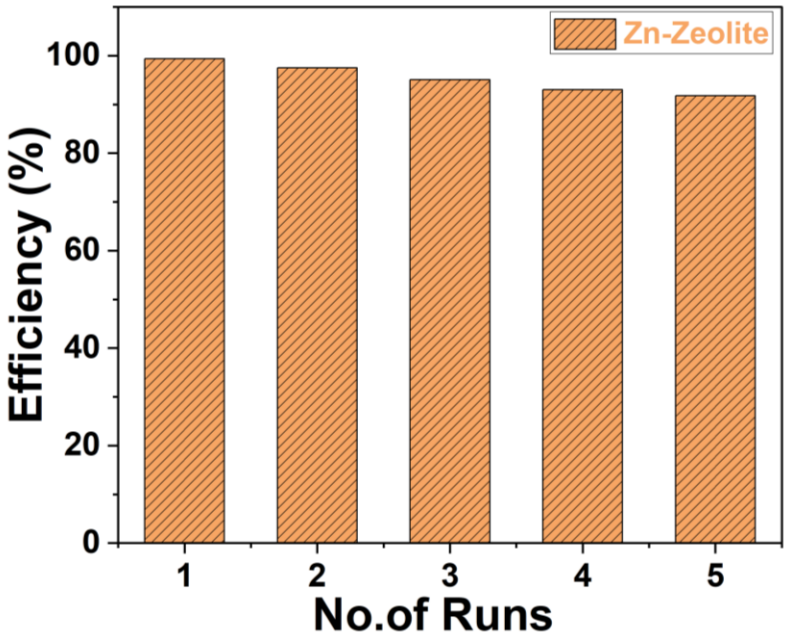

Figure 10 Reusability Test of Zn-Zeolite up to 5 consecutive cycles

4.7 Conclusion

Water contamination is a recurring problem on a global scale. These might be geological or anthropogenic, meaning they were made by humans. The main and most harmful source of water pollution is dye-containing wastewater released by the textile industry. Because dyes are mutagenic and carcinogenic, they can create serious health problems for people. They also cause disturbances to aquatic life, which leads to aquatic animal fatalities. In this work ZnO and Zn-Zeolite were prepared using facile chemical synthesis and checking their potential photo catalytic application in degradation of three dyes methylene blue, methyl orange and Congo red. Zn-Zeolite effectively degrade all three dyes in short period of time. Finally, this photocatalyst can be used as a sustainable catalyst for degradation of dangerous dyes.

4.8 Challenges and Future Directions

Although Zn-doped zeolites have been proven to be high-performance photocatalysts in several reports, some key challenges are discussed below. The most important challenge is the stability of Zn-doped zeolites under long-term photocatalytic conditions. The leaching of zinc ions from zeolite frameworks results in the loss of photocatalytic activity with time.

Consequently, methods for enhancing the Zn-doped zeolites' stability are vital for practical application. The leaching of zinc ions from the frameworks of zeolite leads to the decrease of photocatalytic activity at some point of time (102).

Another challenge is the optimization of the synthesis and characterization methods to allow the uniform distribution and controlled loading of zinc ions into the zeolite framework. This is important to ensure consistent and reproducible photocatalytic performance. Future research directions in this line of work are directed to the exploration of new zeolite frameworks and zinc doping methods that can be used to enhance the photocatalytic activity and stability of Zn-doped zeolites. Further studying the synergistic effects of co-doping with other metals or non-metals can open up new avenues for tailoring the properties of zeolites for specific photocatalytic applications. Areas for further study should include discovering novel zeolite structures and novel ways of zinc doping of zeolites that will increase efficiency of the photocatalytic process and stability of Zn-doped zeolites (103).

In conclusion, Zn-doped zeolites are a promising class of photocatalytic materials that have applications in environmental remediation, energy conversion, and chemical synthesis. This will be achieved only with constant R&D in this sector, leading to the development of more efficient, stable, and sustainable Zn-doped zeolite photocatalysts in the future for a cleaner and greener planet (104).

REFERENCES

1. Ball P. Water is an active matrix of life for cell and molecular biology. Proceedings of the National Academy of Sciences. 2017;114(51):13327-35.
2. Nakayama H, Yamasaki Y, Nakaya S. Effect of hydrogeological structure on geogenic fluoride contamination of groundwater in granitic rock belt in Tanzania. Journal of Hydrology. 2022;612:128026.
3. Qadri H, Bhat RA. The concerns for global sustainability of freshwater ecosystems. Fresh water pollution dynamics and remediation. 2020:1-13.
4. Jayaswal K, Sahu V, Gurjar B. Water pollution, human health and remediation. Water remediation. 2018:11-27.
5. Abbas G, Murtaza B, Bibi I, Shahid M, Niazi NK, Khan MI, et al. Arsenic uptake, toxicity, detoxification, and speciation in plants: physiological, biochemical, and molecular aspects. International journal of environmental research and public health. 2018;15(1):59.
6. Ahrestani Z, Sadeghzadeh S, Emrooz HBM. An overview of atmospheric water harvesting methods, the inevitable path of the future in water supply. RSC advances. 2023;13(15):10273-307.
7. Ahmouda K, Boudiaf M, Benhaoua B. A novel study on the preferential attachment of chromophore and auxochrome groups in azo dye adsorption on different greenly synthesized magnetite nanoparticles: investigation of the influence of the mediating plant extract's acidity. Nanoscale Advances. 2022;4(15):3250-71.
8. Afzal MA, Javed M, Aroob S, Javed T, M. Alnoman M, Alelwani W, et al. The biogenic synthesis of bimetallic Ag/ZnO nanoparticles: a multifunctional approach for methyl violet photocatalytic degradation and the assessment of antibacterial, antioxidant, and cytotoxicity properties. Nanomaterials. 2023;13(14):2079.
9. Vijayaraghavan G, Shanthakumar S. Removal of sulphur black dye from its aqueous solution using alginate from Sargassum sp.(Brown algae) as a coagulant. Environmental Progress & Sustainable Energy. 2015;34(5):1427-34.

10. Zahra M, Yasmeen G, Aftab F, Saleem A, Ambreen S, Malana MA. ZnSe-rGO nanocomposites as photocatalysts for purification of textile dye contaminated water: A green approach to use wastewater for maize cultivation. Heliyon. 2023;9(12).
11. Olas B, Białecki J, Urbańska K, Bryś M. The effects of natural and synthetic blue dyes on human health: A review of current knowledge and therapeutic perspectives. Advances in Nutrition. 2021;12(6):2301-11.
12. Dutta S, Adhikary S, Bhattacharya S, Roy D, Chatterjee S, Chakraborty A, et al. Contamination of textile dyes in aquatic environment: Adverse impacts on aquatic ecosystem and human health, and its management using bioremediation. Journal of Environmental Management. 2024;353:120103.
13. Roy M, Saha R. Dyes and their removal technologies from wastewater: A critical review. Intelligent environmental data monitoring for pollution management. 2021:127-60.
14. Sharma S, Khare N. Hierarchical Bi2S3 nanoflowers: A novel photocatalyst for enhanced photocatalytic degradation of binary mixture of Rhodamine B and Methylene blue dyes and degradation of mixture of p-nitrophenol and p-chlorophenol. Advanced Powder Technology. 2018;29(12):3336-47.
15. Solayman H, Hossen MA, Abd Aziz A, Yahya NY, Leong KH, Sim LC, et al. Performance evaluation of dye wastewater treatment technologies: A review. Journal of Environmental Chemical Engineering. 2023;11(3):109610.
16. Bal G, Thakur A. Distinct approaches of removal of dyes from wastewater: A review. Materials Today: Proceedings. 2022;50:1575-9.
17. Baldev E, MubarakAli D, Ilavarasi A, Pandiaraj D, Ishack KSS, Thajuddin N. Degradation of synthetic dye, Rhodamine B to environmentally non-toxic products using microalgae. Colloids and Surfaces B: Biointerfaces. 2013;105:207-14.
18. Piaskowski K, Świderska-Dąbrowska R, Zarzycki PK. Dye removal from water and wastewater using various physical, chemical, and biological processes. Journal of AOAC International. 2018;101(5):1371-84.
19. Dawood S, Sen T. Review on dye removal from its aqueous solution into alternative cost effective and non-conventional adsorbents. Journal of Chemical and Process Engineering. 2014;1(104):1-11.
20. Ledakowicz S, Paździor K. Recent achievements in dyes removal focused on advanced oxidation processes integrated with biological methods. Molecules. 2021;26(4):870.
21. Martínez-Sánchez C, Robles I, Godínez L. Review of recent developments in electrochemical advanced oxidation processes: application to remove dyes, pharmaceuticals, and pesticides. International Journal of Environmental Science and Technology. 2022;19(12):12611-78.
22. Peramune D, Manatunga DC, Dassanayake RS, Premalal V, Liyanage RN, Gunathilake C, et al. Recent advances in biopolymer-based advanced oxidation processes for dye removal applications: A review. Environmental Research. 2022;215:114242.
23. Saeed M, Muneer M, Haq Au, Akram N. Photocatalysis: an effective tool for photodegradation of dyes—a review. Environmental Science and Pollution Research. 2022;29(1):293-311.
24. Zhang T, Liu Y, Zhong S, Zhang L. AOPs-based remediation of petroleum hydrocarbons-contaminated soils: Efficiency, influencing factors and environmental impacts. Chemosphere. 2020;246:125726.
25. Chiu Y-H, Chang T-FM, Chen C-Y, Sone M, Hsu Y-J. Mechanistic insights into photodegradation of organic dyes using heterostructure photocatalysts. Catalysts. 2019;9(5):430.
26. Sharma J, Dhiman P, Alshgari RA, ALOthman ZA, Kumar A, Sharma G, et al.

Advances in photocatalytic environmental and clean energy applications of Bismuth-rich oxy halides (BixOyXz) based heterojunctions: A review. Materials Today Sustainability. 2023:100327.
27. Qin Z, Melinte G, Gilson JP, Jaber M, Bozhilov K, Boullay P, et al. The mosaic structure of zeolite crystals. Angewandte Chemie. 2016;128(48):15273-6.
28. Smeets S, Zou X. Zeolite structures. 2017.
29. Murthy NS. Scattering techniques for structural analysis of biomaterials. Characterization of Biomaterials: Elsevier; 2013. p. 34-72.
30. Xiong M, Zhao X, Yin G, Ching W-Y, Li N. Unraveling the effects of linker substitution on structural, electronic and optical properties of amorphous zeolitic imidazolate frameworks-62 (a-ZIF-62) glasses: a DFT study. RSC advances. 2020;10(24):14013-24.
31. Wang Y, Bryant SH, Cheng T, Wang J, Gindulyte A, Shoemaker BA, et al. Pubchem bioassay: 2017 update. Nucleic acids research. 2017;45(D1):D955-D63.
32. Anucha CB, Altin I, Bacaksiz E, Stathopoulos VN. Titanium dioxide (TiO_2)-based photocatalyst materials activity enhancement for contaminants of emerging concern (CECs) degradation: In the light of modification strategies. Chemical Engineering Journal Advances. 2022;10:100262.
33. Rakanović M, Vukojević A, Savanović MM, Armaković S, Pelemiš S, Živić F, et al. Zeolites as adsorbents and photocatalysts for removal of dyes from the aqueous environment. Molecules. 2022;27(19):6582.
34. Alakhras F, Alhajri E, Haounati R, Ouachtak H, Addi AA, Saleh TA. A comparative study of photocatalytic degradation of Rhodamine B using natural-based zeolite composites. Surfaces and Interfaces. 2020;20:100611.
35. Li Y, Yu J. New stories of zeolite structures: their descriptions, determinations, predictions, and evaluations. Chemical reviews. 2014;114(14):7268-316.
36. Georgiev D, Bogdanov B, Markovska I, Hristov Y. A study on the synthesis and structure of zeolite NaX. Journal of Chemical Technology and Metallurgy. 2013;48(2):168-73.
37. Mansouri M, Mozafari N, Bayati B, Setareshenas N. Photo-catalytic dye degradation of methyl orange using zirconia–zeolite nanoparticles. Bulletin of Materials Science. 2019;42:1-11.
38. Swain J, Priyadarshini A, Hajra S, Panda S, Panda J, Samantaray R, et al. Photocatalytic dye degradation by BaTiO3/zeolitic imidazolate framework composite. Journal of Alloys and Compounds. 2023;965:171438.
39. Nassar MY, Abdelrahman EA. Hydrothermal tuning of the morphology and crystallite size of zeolite nanostructures for simultaneous adsorption and photocatalytic degradation of methylene blue dye. Journal of Molecular Liquids. 2017;242:364-74.
40. Badvi K, Javanbakht V. Enhanced photocatalytic degradation of dye contaminants with TiO2 immobilized on ZSM-5 zeolite modified with nickel nanoparticles. Journal of Cleaner Production. 2021;280:124518.
41. You-ji L, Wei C. Photocatalytic degradation of Rhodamine B using nanocrystalline TiO 2–zeolite surface composite catalysts: effects of photocatalytic condition on degradation efficiency. Catalysis Science & Technology. 2011;1(5):802-9.
42. Mohamed F, Hassaballa S, Shaban M, Ahmed AM. Highly efficient photocatalyst fabricated from the chemical recycling of iron waste and natural zeolite for super dye degradation. Nanomaterials. 2022;12(2):235.
43. Mahamud M, Taddesse AM, Bogale Y, Bezu Z. Zeolite supported CdS/TiO2/CeO2 composite: Synthesis, characterization and photocatalytic activity for methylene blue dye degradation. Materials Research Bulletin. 2023;161:112176.
44. Sodha V, Koshti H, Gaur R, Ahmad I, Bandyopadhyay R, Shahabuddin S. Synthesis

of zeolite-doped polyaniline composite for photocatalytic degradation of methylene blue from aqueous solution. Environmental Science and Pollution Research. 2023;30(16):46159-74.
45. Pambudi FI, Prasetyo N. Theoretical investigation on the structure of mixed-metal zeolitic imidazolate framework and its interaction with CO2. Computational Materials Science. 2022;210:111033.
46. Madsen RS, Stepniewska M, Yang Y, Qiao A, Winters WM, Zhou C, et al. Mixed metal node effect in zeolitic imidazolate frameworks. RSC advances. 2022;12(17):10815-24.
47. Baburin IA, Leoni S. The energy landscapes of zeolitic imidazolate frameworks (ZIFs): towards quantifying the presence of substituents on the imidazole ring. Journal of Materials Chemistry. 2012;22(20):10152-4.
48. Baghban A, Habibzadeh S, Ashtiani FZ. Bandgaps of noble and transition metal/ZIF-8 electro/catalysts: a computational study. RSC advances. 2020;10(39):22929-38.
49. Zhang H, Shi Q, Kang X, Dong J. Vapor-assisted conversion synthesis of prototypical zeolitic imidazolate framework-8. Journal of Coordination Chemistry. 2013;66(12):2079-90.
50. Zhou K, Mousavi B, Luo Z, Phatanasri S, Chaemchuen S, Verpoort F. Characterization and properties of Zn/Co zeolitic imidazolate frameworks vs. ZIF-8 and ZIF-67. Journal of Materials Chemistry A. 2017;5(3):952-7.
51. Butler KT, Worrall SD, Molloy CD, Hendon CH, Attfield MP, Dryfe RA, et al. Electronic structure design for nanoporous, electrically conductive zeolitic imidazolate frameworks. Journal of Materials Chemistry C. 2017;5(31):7726-31.
52. Kim YJ, Kim M-Z, Alam SF, ur Rehman A, Devipriyanka A, Sharma P, et al. Polarity-dependent particle size of zeolitic imidazolate framework synthesized in various solvents. Materials Chemistry and Physics. 2021;259:124021.
53. Newman MD, Stotland M, Ellis JI. The safety of nanosized particles in titanium dioxide–and zinc oxide–based sunscreens. Journal of the American Academy of Dermatology. 2009;61(4):685-92.
54. Cross SE, Innes B, Roberts MS, Tsuzuki T, Robertson TA, McCormick P. Human skin penetration of sunscreen nanoparticles: in-vitro assessment of a novel micronized zinc oxide formulation. Skin pharmacology and physiology. 2007;20(3):148-54.
55. Gupta M, Mahajan VK, Mehta KS, Chauhan PS. Zinc therapy in dermatology: a review. Dermatology research and practice. 2014;2014(1):709152.
56. Mohammed YH, Holmes A, Haridass IN, Sanchez WY, Studier H, Grice JE, et al. Support for the safe use of zinc oxide nanoparticle sunscreens: lack of skin penetration or cellular toxicity after repeated application in volunteers. Journal of Investigative Dermatology. 2019;139(2):308-15.
57. Tymoszuk A, Wojnarowicz J. Zinc oxide and zinc oxide nanoparticles impact on in vitro germination and seedling growth in Allium cepa L. Materials. 2020;13(12):2784.
58. Sirelkhatim A, Mahmud S, Seeni A, Kaus NHM, Ann LC, Bakhori SKM, et al. Review on zinc oxide nanoparticles: antibacterial activity and toxicity mechanism. Nano-micro letters. 2015;7:219-42.
59. Jiang J, Pi J, Cai J. The advancing of zinc oxide nanoparticles for biomedical applications. Bioinorganic chemistry and applications. 2018;2018(1):1062562.
60. Jones N, Ray B, Ranjit KT, Manna AC. Antibacterial activity of ZnO nanoparticle suspensions on a broad spectrum of microorganisms. FEMS microbiology letters. 2008;279(1):71-6.
61. Bakhori SKM, Mahmud S, Azaldin NQ, Nadzri NFNM, Zakaria S, Chuan HT, et al. Characterisation and larvicidal effects of different zinc oxide nanoparticles against Aedes aegypti larvae. Materials Today: Proceedings. 2023.
62. Qi K, Cheng B, Yu J, Ho W. Review on the improvement of the photocatalytic and antibacterial activities of ZnO. Journal of Alloys and Compounds. 2017;727:792-820.

63. Król A, Pomastowski P, Rafińska K, Railean-Plugaru V, Buszewski B. Zinc oxide nanoparticles: Synthesis, antiseptic activity and toxicity mechanism. Advances in colloid and interface science. 2017;249:37-52.
64. Anjum S, Hashim M, Malik SA, Khan M, Lorenzo JM, Abbasi BH, et al. Recent advances in zinc oxide nanoparticles (ZnO NPs) for cancer diagnosis, target drug delivery, and treatment. Cancers. 2021;13(18):4570.
65. Naser SS, Ghosh B, Simnani FZ, Singh D, Choudhury A, Nandi A, et al. Emerging trends in the application of green synthesized biocompatible ZnO nanoparticles for translational paradigm in cancer therapy. Journal of Nanotheranostics. 2023;4(3):248-79.
66. Eppler RA. Ceramic Coatings. 2012.
67. Czyżowska A, Barbasz A. A review: zinc oxide nanoparticles–friends or enemies? International journal of environmental health research. 2022;32(4):885-901.
68. Beeby SP, Tudor MJ, White N. Energy harvesting vibration sources for microsystems applications. Measurement science and technology. 2006;17(12):R175.
69. Liu Y, Li Y, Pan B, Zhang X, Zhang H, Steinberg CE, et al. Application of low dosage of copper oxide and zinc oxide nanoparticles boosts bacterial and fungal communities in soil. Science of the Total Environment. 2021;757:143807.
70. Asmatulu R. Nanocoatings for corrosion protection of aerospace alloys. Corrosion protection and control using nanomaterials: Elsevier; 2012. p. 357-74.
71. Zhang L, Ma A, Jiang J, Song D, Chen J, Yang D. Anti-corrosion performance of waterborne Zn-rich coating with modified silicon-based vehicle and lamellar Zn (Al) pigments. Progress in Natural Science: Materials International. 2012;22(4):326-33.
72. Kumar N, Sharma A. Surface Coatings and Functionalization Strategies for Corrosion Mitigation. Functionalized Nanomaterials for Corrosion Mitigation: Synthesis, Characterization, and Applications: ACS Publications; 2022. p. 291-316.
73. Wang H, Di D, Zhao Y, Yuan R, Zhu Y. A multifunctional polymer composite coating assisted with pore-forming agent: preparation, superhydrophobicity and corrosion resistance. Progress in Organic Coatings. 2019;132:370-8.
74. Gondek J, Babinec M, Kusý M. The corrosion performance of Zn-Al-Mg based alloys with tin addition in neutral salt spray environment. J Achiev Mater Manuf Eng. 2015;70:70-7.
75. Almeida Streitwieser D, Arteaga A, Gallo-Cordova A, Hidrobo A, Ponce S. Chemical recycling of used motor oil by catalytic cracking with metal-doped aluminum silicate catalysts. Sustainability. 2023;15(13):10522.
76. Boidot A, Gheno F, Bentiss F, Jama C, Vogt J-B. Effect of aluminum flakes on corrosion protection behavior of water-based hybrid zinc-rich coatings for carbon steel substrate in NaCl environment. Coatings. 2022;12(10):1390.
77. Feng Y, Li T, Ge K, Wang X, Wen G, Ye J, et al. Impedance matching strategy boost excellent wave absorption performance of zinc-Aluminosilicate cladded short carbon fiber core-sheath structure. Materials Research Bulletin. 2022;153:111872.
78. Gayatri R, Agustina TE, Bahrin D, Moeksin R, Gustini G. Preparation and characterization of ZnO-zeolite nanocomposite for photocatalytic degradation by ultraviolet light. Journal of Ecological Engineering. 2021;22(2):178-86.
79. Zhi Y, Yi Y, Deng C, Zhang Q, Yang S, Peng F. Defect-Enriched ZnO/ZnS Heterostructures Derived from Hydrozincite Intermediates for Hydrogen Evolution under Visible Light. ChemSusChem. 2022;15(18):e202200860.
80. Zhang Z, Lu N, Cai W, Wen J, Li K, Qu H. A novel Zn-doped CHA zeolite coupled CDs for photocatalytic nitrogen fixation. Molecular Catalysis. 2023;549:113471.
81. Limón-Rocha I, Guzmán-González CA, Anaya-Esparza LM, Romero-Toledo R, Rico JL, González-Vargas OA, et al. Effect of the precursor on the synthesis of ZnO and its photocatalytic activity. Inorganics. 2022;10(2):16.

82. Khaleque A, Alam MM, Hoque M, Mondal S, Haider JB, Xu B, et al. Zeolite synthesis from low-cost materials and environmental applications: A review. Environmental advances. 2020;2:100019.
83. Ackley MW, Rege SU, Saxena H. Application of natural zeolites in the purification and separation of gases. Microporous and Mesoporous Materials. 2003;61(1-3):25-42.
84. Yuan E, Han W, Zhang G, Zhao K, Mo Z, Lu G, et al. Structural and Textural Characteristics of Zn-Containing ZSM-5 Zeolites and Application for the Selective Catalytic Reduction of NO x with NH 3 at High Temperatures. Catalysis Surveys from Asia. 2016;20:41-52.
85. Ahmad M, Zhu J. ZnO based advanced functional nanostructures: synthesis, properties and applications. Journal of Materials chemistry. 2011;21(3):599-614.
86. Maier SM. New Insights on Fe-zeolite Catalysts for the Reduction of NO X with NH 3: Technische Universität München; 2011.
87. Kumar S, Kumar A, Kumar A, Krishnan V. Nanoscale zinc oxide based heterojunctions as visible light active photocatalysts for hydrogen energy and environmental remediation. Catalysis Reviews. 2020;62(3):346-405.
88. Askari N, Beheshti M, Mowla D, Farhadian M. Synthesis of CuWO4/Bi2S3 Z-scheme heterojunction with enhanced cephalexin photodegradation. Journal of Photochemistry and Photobiology A: Chemistry. 2020;394:112463.
89. Setthaya N, Chindaprasirt P, Yin S, Pimraksa K. TiO2-zeolite photocatalysts made of metakaolin and rice husk ash for removal of methylene blue dye. Powder Technology. 2017;313:417-26.
90. Haounati R, Alakhras F, Ouachtak H, Saleh TA, Al-Mazaideh G, Alhajri E, et al. Synthesized of zeolite@ Ag2O nanocomposite as superb stability photocatalysis toward hazardous rhodamine B dye from water. Arabian Journal for Science and Engineering. 2023;48(1):169-79.
91. Wardhani S, Rahman MF, Purwonugroho D, Tjahjanto RT, Damayanti CA, Wulandari IO. Photocatalytic degradation of methylene blue using TiO2-natural zeolite as a photocatalyst. J Pure Appl Chem Res. 2016;5(1):19-27.
92. Girma S, Taddesse AM, Bogale Y, Bezu Z. Zeolite-supported g-C3N4/ZnO/CeO2 nanocomposite: Synthesis, characterization and photocatalytic activity study for methylene blue dye degradation. Journal of Photochemistry and Photobiology A: Chemistry. 2023;444:114963.
93. Chakraborty A, Islam DA, Acharya H. Facile synthesis of CuO nanoparticles deposited zeolitic imidazolate frameworks (ZIF-8) for efficient photocatalytic dye degradation. Journal of Solid State Chemistry. 2019;269:566-74.
94. Hussain SM, Hussain T, Faryad M, Ali Q, Ali S, Rizwan M, et al. Emerging aspects of photo-catalysts (TiO2 & ZnO) doped zeolites and advanced oxidation processes for degradation of azo dyes: a review. Current Analytical Chemistry. 2021;17(1):82-97.
95. Wang L-Q, Li H-J, Diao J-Q, Hou D-D, Qiang M-M, Chen L-J. Photocatalytic performance of hierarchical metal-doped framework zeolite. Inorganic Chemistry Communications. 2022;140:109425.
96. Hutsul K, Ivanenko I, Patrylak L, Pertko O, Kamenskyh D. ZnO/Zeolite composite photocatalyst for dyes degradation. Applied Nanoscience. 2023;13(12):7601-9.
97. Kottegoda N, Munaweera I, Madusanka N, Karunaratne V. A green slow-release fertilizer composition based on urea-modified hydroxyapatite nanoparticles encapsulated wood. Current science. 2011:73-8.
98. Naseem F, Zhi Y, Farrukh MA, Hussain F, Yin Z. Mesoporous ZnAl2Si10O24 nanofertilizers enable high yield of Oryza sativa L. Scientific Reports. 2020;10(1):10841.
99. Kant S, Kumar A. A comparative analysis of structural, optical and photocatalytic

properties of ZnO and Ni doped ZnO nano spheres prepared by sol gel method. Adv Mat Let. 2012;3(4):350-4.
100. Abhilash MR, Akshatha G, Srikantaswamy S. Photocatalytic dye degradation and biological activities of the Fe 2 O 3/Cu 2 O nanocomposite. RSC advances. 2019;9(15):8557-68.
101. Singha MK, Patra A, Rojwal V, Deepa K. Single-step fabrication of ZnO microflower thin films for highly efficient and reusable photocatalytic activity. Journal of Materials Science: Materials in Electronics. 2020;31(16):13578-87.
102. Samara F, Ghalayini T, Abu Farha N, Kanan S. The photocatalytic degradation of 2, 3, 7, 8-tetrachlorodibenzo-p-dioxin in the presence of silver–titanium based catalysts. Catalysts. 2020;10(9):957.
103. Wang C-C, Zhang Y-Q, Li J, Wang P. Photocatalytic CO2 reduction in metal–organic frameworks: a mini review. Journal of Molecular Structure. 2015;1083:127-36.
104. Dhaka S, Kumar R, Deep A, Kurade MB, Ji S-W, Jeon B-H. Metal–organic frameworks (MOFs) for the removal of emerging contaminants from aquatic environments. Coordination Chemistry Reviews. 2019;380:330-52.